ARTICLE IN PRESS
YNIMG-10472; No. of pages: 21; 4C: 6, 7, 8, 9, 10, 11, 12, 13, 14, 15, 16, 17
NeuroImage xxx (2013) xxx–xxx
Contents lists available at SciVerse ScienceDirect
NeuroImage
journal homepage: www.elsevier.com/locate/ynimg

Review

Function in the human connectome: Task-fMRI and individual differences in behavior

Deanna M. Barch [a,b,c,*], Gregory C. Burgess [d], Michael P. Harms [b], Steven E. Petersen [a,c,d,e], Bradley L. Schlaggar [c,d,e,f], Maurizio Corbetta [c,d,e], Matthew F. Glasser [d], Sandra Curtiss [d], Sachin Dixit [b], Cindy Feldt [b], Dan Nolan [b], Edward Bryant [b], Tucker Hartley [b], Owen Footer [b], James M. Bjork [g], Russ Poldrack [h,i], Steve Smith [j], Heidi Johansen-Berg [j], Abraham Z. Snyder [c], David C. Van Essen [d], for the WU-Minn HCP Consortium

[a] Department of Psychology, Washington University, St. Louis, MO, USA
[b] Department of Psychiatry, Washington University School of Medicine, St. Louis, MO, USA
[c] Department of Radiology, Washington University School of Medicine, St. Louis, MO, USA
[d] Department of Anatomy and Neurobiology, Washington University School of Medicine, St. Louis, MO, USA
[e] Department of Neurology, Washington University School of Medicine, St. Louis, MO, USA
[f] Department of Pediatrics, Washington University School of Medicine, St. Louis, MO, USA
[g] Division of Clinical Neuroscience and Behavioral Research, National Institute on Drug Abuse, National Institutes of Health, Bethesda, MD, USA
[h] Department of Psychology, University of Texas, Austin, TX, USA
[i] Department of Neuroscience and Imaging Research Center, University of Texas, Austin, TX, USA
[j] Centre for Functional MRI of the Brain (FMRIB), Oxford University, Oxford, UK

ARTICLE INFO

Article history:
Accepted 3 May 2013
Available online xxxx

Keywords:
Cognitive
Emotion
Sensory and motor function
Individual differences
Task-fMRI
Personality
Connectivity

ABSTRACT

The primary goal of the Human Connectome Project (HCP) is to delineate the typical patterns of structural and functional connectivity in the healthy adult human brain. However, we know that there are important individual differences in such patterns of connectivity, with evidence that this variability is associated with alterations in important cognitive and behavioral variables that affect real world function. The HCP data will be a critical stepping-off point for future studies that will examine how variation in human structural and functional connectivity play a role in adult and pediatric neurological and psychiatric disorders that account for a huge amount of public health resources. Thus, the HCP is collecting behavioral measures of a range of motor, sensory, cognitive and emotional processes that will delineate a core set of functions relevant to understanding the relationship between brain connectivity and human behavior. In addition, the HCP is using task-fMRI (tfMRI) to help delineate the relationships between individual differences in the neurobiological substrates of mental processing and both functional and structural connectivity, as well as to help characterize and validate the connectivity analyses to be conducted on the structural and functional connectivity data. This paper describes the logic and rationale behind the development of the behavioral, individual difference, and tfMRI batteries and provides preliminary data on the patterns of activation associated with each of the fMRI tasks, at both group and individual levels.

Introduction

The primary goal of the Human Connectome Project (HCP) is to delineate the patterns of structural and functional connectivity in the healthy adult human brain and to provide these data as public resource for biomedical research. However, we know that there are important individual differences in such patterns of connectivity even among persons with no diagnosable neurological or psychiatric disorders, and there is increasing evidence that this variability is associated with alterations in cognitive and behavioral variables that constrain real world function (Bassett et al., 2009; Song et al., 2008; van den Heuvel et al., 2009). For example, higher IQ among healthy adults is associated with shorter path length and higher global efficiency in measures of brain functional connectivity (Li et al., 2009) as well as greater global connectivity in prefrontal cortex (Cole et al., 2012), thus providing evidence that more efficient connectivity contributes to more effective cognitive function. As another example, developmental research is increasingly suggesting that maturation of functional and structural networks in the human brain underlies key aspects of cognitive and emotional development (Fair et al., 2007, 2009; Hwang et al., 2012; Imperati et al., 2011; Stevens et al., 2009; Supekar et al., 2009; Zuo et al., 2010).

* Corresponding author at: Departments of Psychology, Psychiatry and Radiology, Washington University, Box 1125, One Brookings Drive, St. Louis, MO 63130, USA. Fax: +1 314 935 8790.
E-mail address: dbarch@artsci.wustl.edu (D.M. Barch).

1053-8119/$ – see front matter © 2013 Published by Elsevier Inc.
http://dx.doi.org/10.1016/j.neuroimage.2013.05.033

The data to be collected on healthy adults in the Human Connectome Project will be a critical stepping-off point for future studies that will examine how variation in human structural and functional connectivity play a role in adult and pediatric neurological and psychiatric disorders that collectively incur a huge economic cost to the country of the US (e.g., estimated $320 billion in 2002 alone) (Insel, 2008). Indeed, an extensive empirical literature already provides evidence for impairments in both structural and functional connectivity in psychiatric disorders such as autism (Vissers et al., 2012), schizophrenia (Fitzsimmons et al., 2013; Fornito et al., 2012; Repovs et al., 2011; Whitfield-Gabrieli and Ford, 2012), ADHD (Fair et al., 2012), mood disorders (Hulvershorn et al., 2011; Strakowski et al., 2012), addiction (Sutherland et al., 2012), neurological disorders such as stroke (Carter et al., 2010; He et al., 2007), Tourette syndrome (Church et al., 2009; Worbe et al., 2012) and multiple sclerosis (Hawellek et al., 2011; He et al., 2009; Rocca et al., 2009; Schoonheim et al., 2013), and the cognitive consequences of prematurity (Constable et al., 2008; Gozzo et al., 2009; Mullen et al., 2011; Panigrahy et al., 2012; Schafer et al., 2009). Thus, a critical component of the HCP is collecting behavioral measures of a range of motor, sensory, cognitive and emotional processes that will delineate a core set of functions relevant to understanding the relationship between brain connectivity and human function. Another critical component of the HCP is to use task-fMRI (tfMRI) to help delineate the relationships between individual differences in the neurobiological substrates of cognitive and affective processing and both functional and structural connectivity. tfMRI data will also help characterize and validate the connectivity analyses to be conducted on the structural and resting-state functional data. The goal of this paper is to describe the logic and rationale behind the development of the behavioral, individual differences and tfMRI batteries and to provide preliminary data on the patterns of activation associated with each of the fMRI tasks, at both group and individual levels.

Individual differences in the Human Connectome Project

Our goal was to identify and utilize a reliable and well-validated battery of measures that assess a wide range of human functions and behaviors in a reasonable amount of time (3–4 h total, to satisfy subject burden considerations). As requested by the NIH Request for Applications for the Human Connectome Project, the base for our assessment of human behavior is the set tools and methods developed by the Blueprint-funded NIH Toolbox for Assessment of Neurological and Behavioral function (http://www.nihtoolbox.org), which was designed to generate an efficient and comprehensive battery of assessment tools for projects exactly like the HCP. The NIH Toolbox includes measures of cognitive, emotional, motor and sensory processes that were selected based on a consensus building process and were designed to be used in healthy individuals between the ages of 3 and 85 years. These tasks were developed and validated using assessment methodologies that included item response theory and Computer Adaptive Testing where appropriate and feasible. Based on discussions with our External Advisory Board, and interactions among the members of the consortium, we expanded the battery of HCP behavioral tests to include measures of the following domains not covered by the Toolbox: 1) subthreshold symptoms of mood, anxiety, and substance abuse — information we thought would be of great interest to researchers using this database to generate and test predictions about variations in behaviors and symptoms relevant to psychiatric, substance and neurological disorders; 2) additional measures of visual, memory and emotion processing; 3) personality; 4) delay discounting (as a measure of self-regulation and neuroeconomic decision making) (Dalley et al., 2008; Shamosh et al., 2008); 5) fluid intelligence as a measure of higher-order relational reasoning that has been linked to important individual differences in both life function and brain function (Burgess et al., 2011); 6) menstrual cycle and hormonal function for women; and 7) sleep function, which may be highly relevant to understanding individual differences in behavior. Task selection also reflected the preferences of the NIH Human Connectome Project Team (program officials of the participating NIH Blueprint Institutes and Centers), as voiced by the NIH Scientific Officer of the project, Dr. James Bjork. Each of these assessments is described in more detail below.

To illustrate how these data might be used to examine the behavioral relevance of individual differences in functional or structural connectivity, investigators will be able to (for example) examine how variation in scores on the NIH Toolbox working memory task relates to variation in: 1) the amplitude of spontaneous resting-state fluctuations in time series associated with individual functional parcels from whole-brain parcellation; 2) connection strengths between network nodes (parcels), such as will be estimated via a) full or partial correlation matrices derived from the time series associated with whole-brain parcellation of rfMRI data, and/or b) probabilistic tractography estimated between different nodes from dMRI data; 3) ICA component spatial maps identified in the resting state data, or task based activation data during the working memory task; 4) connectivity metrics associated with specific regions of interest to working memory (e.g., superior parietal cortex); or 5) connectivity metrics associated with "hub" or "rich club" regions (Buckner et al., 2009; Collin et al., 2013; Harriger et al., 2012; van den Heuvel and Sporns, 2011). As another example, investigators will be able to examine how variation in personality variables such as extroversion or neuroticism relate to variation in the kinds of connectivity measures described above, including connectivity metrics associated with specific regions of interest to neuroticism or extroversion (e.g., amygdala and caudate).

tfMRI in the Human Connectome Project

Our primary goals in including tfMRI in the HCP were to: 1) help identify as many "nodes" as possible that can guide, validate and interpret the results of the connectivity analyses that will be conducted on resting state fMRI (R-fMRI), resting state MEG (R-MEG) and diffusion data; 2) to allow a comparison of network connectivity in a task context to connectivity results generated using R-fMRI; and 3) to relate signatures of activation magnitude or location in key network nodes to individual differences in performance, psychometric measures, or other phenotypic traits. To accomplish these goals, we developed a battery of tasks that can identify node locations in as wide a range of neural systems as is feasible within realistic time constraints. These "functional localizers" will: 1) aid in the identification of nodes that will be used in analyses of network structure; 2) help validate/interpret the location of functional areas identified in the R-fMRI analyses; and 3) provide a comparative metric for examining how individual differences in behavioral and genetic measures relate to individual differences in functional and structural connectivity measures. A subset of these tasks will be combined with T-MEG to allow analyses of the flow of information among the nodes identified in key networks at a much finer timescale than possible with BOLD fMRI (see Larson-Prior et al., this issue).

There are numerous ways in which the regions of activation identified in the tfMRI data could be used to facilitate the examination and interpretation of the functional and structural connectivity data. Some examples that the HCP has discussed include: 1) using peaks identified in the task data as validation for parcellation schemes used on the resting state connectivity data or diffusion data (e.g., do peaks fall in areas identified as low transition points between areal boundaries (Cohen et al., 2008; Nelson et al., 2010); 2) using peaks identified in the task data to subdivide regions identified in the resting state connectivity data (e.g., when there are different peaks from different task domains located within a larger "region" identified with resting state connectivity data); 3) examining whether boundaries of regional activations identified in the tfMRI data map to boundaries identified by other methods (e.g., rsfMRI and myelin maps); 4) examining whether parcellation results from task-based

Please cite this article as: Barch, D.M., et al., Function in the human connectome: Task-fMRI and individual differences in behavior, NeuroImage (2013), http://dx.doi.org/10.1016/j.neuroimage.2013.05.033

connectivity data correspond to results from resting state data or diffusion data; or 4) using peaks from task data as input to seed-based connectivity or tract tracing approaches. We are confident that other investigators will identify additional creative and innovative ways in which the tfMRI data can be used to help guide, validate and interpret the functional and structural connectivity data.

Our choice of tfMRI tasks was driven by the following considerations. We aimed to identify nodes: 1) in *well-characterized* neural systems; 2) in as *wide a range* of neural systems as possible (e.g., cortical and subcortical; primary sensory, higher level cognitive and emotional regions); 3) with activation locations that are *reliable* over time in individual subjects; 4) with activations consistently detectable in most individuals (*sensitivity*); and 5) that are associated with a broad range of cognitive and affective processes of interest to the NIH Blueprint Institutes. In addition, it was necessary that a subset of the tasks must be suitable for T-MEG. Like the expanded HCP behavioral battery, the domains examined for tfMRI were chosen based on discussions with our External Advisory Board, interactions among the members of the consortium, and the preferences of the NIH Human Connectome Project Team, as voiced by the NIH Scientific Officer of the project, Dr. James Bjork. Our initial piloting targeted a broad range of domains that sampled diverse neural systems of interest to a wide range of investigators, including: 1) visual and somatosensory–motor systems; 2) category-specific representations; 3) language function (semantic and phonological processing); 4) attention systems; 5) working memory/cognitive control systems; 6) emotion processing; 7) decision-making/reward processing; and 8) episodic memory systems. Table 1 lists the candidate tasks and domains that drove our initial pilot testing. This table includes information on the relevant processing domain/neural systems, exemplar regions reported to be activated in the tasks, citations providing empirical evidence of their utility as functional localizers in individual subjects, and any existing evidence regarding their test–retest reliability. As described in the Methods, there were (are) two phases to the HCP (also see Van Essen et al., 2012, in press)). As described in more detail in the Methods, phase I of the HCP involved a broad array of pilot testing for pulse sequences, hardware, software and task paradigms (both in and out of the scanner). During this pilot testing, we optimized the length and design of the tasks, compared different paradigms for assessing similar functions and brain networks, and examined the degree of unique brain coverage provided by the different tasks. Phase II is ongoing and involves data acquisition on a large sample of extended twin sibships (Van Essen et al., 2012, in press) using the paradigms and pulse sequences optimized in Phase I. Phase II will generate a publicly available database on normative patterns of structural and functional brain connectivity, and relationships to individual differences in cognition, emotion, and function.

Table 1
Candidate task domains for task-FMRI in the Human Connectome Project.

Domain(s)	Task	Regions of interest
Visual, somatosensory motor • Localizer: (Drobyshevsky et al., 2006; Gountouna et al., 2009; Hirsch et al., 2000); reliable across subjects (Drobyshevsky et al., 2006; Hirsch et al., 2000) and time (Warnking et al., 2002)	Retinotopic mapping Finger responses	Primary motor; premotor; striatum; retinotopic visual areas
Category-specific representations • Localizer: (Downing et al., 2001; Fox et al., 2009; Peelen and Downing, 2005; Taylor et al., 2007); reliable across subjects (Downing et al., 2001; Fox et al., 2009) and time (Kung et al., 2007; Peelen and Downing, 2005)	Alternating blocks of 0-back and 2-back working memory; faces, non-living man-made objects, animals, body parts, houses, or words.	Fusiform; occipital face areas; superior temporal sulcus; lateral occipital; parahippocampal gyrus; visual word form area
Working memory; cognitive control • Localizer: (Drobyshevsky et al., 2006); reliable across subjects (Drobyshevsky et al., 2006) and time (Caceres et al., 2009)	N-back task (2-back versus 0-back) embedded in category specific representation task	Dorsolateral + anterior prefrontal; inferior frontal; precentral gyrus; anterior cingulate; dorsal parietal
Dorsal and ventral attention systems • Reliable across subjects and robust activation in fMRI (Doricchi et al., 2010; Engelmann et al., 2009)	Variant of Posner task (compare blocked and event-related versions)	Frontal eye fields; supplementary eye fields; precuneus; intraparietal sulcus: anterior, posterior cingulate
Language processing • Reliable across subjects (Binder et al., 2011) and robust activation in both fMRI and ERP (Ditman et al., 2007; Kuperberg et al., 2008)	1) Auditory sentence presentation with detection of semantic, syntactic and pragmatic violations; versus 2) auditory story presentation with comprehension questions versus math problems	Inferior frontal; superior temporal; anterior cingulate
Emotion processing • Localizer: (Drobyshevsky et al., 2006; Phan et al., 2004); reliable across subjects (Drobyshevsky et al., 2006; Phan et al., 2004) and time (Manuck et al., 2007), robust activation in fMRI (Hariri et al., 2002)	1) Valence judgments (negative and neutral pictures from IAPS) versus 2) Hariri Hammer Task	Amygdala; hippocampus; insula; medial prefrontal
Memory • Localizer: (Miller et al., 2002, 2009); reliable across subjects (Miller et al., 2002, 2009) and time (Miller et al., 2002, 2009)	Remember, know, new recognition judgments on category-specific task stimuli	Parietal; hippocampus; entorhinal cortex
Reward & decision making • Reliable across subjects and robust activation in fMRI (Delgado et al., 2000; Forbes et al., 2009; May et al., 2004; Tricomi et al., 2004)	Gambling decision making task (compare blocked and event-related versions)	Striatum; ventral medial prefrontal; orbitofrontal
Social cognition • Reliable across subjects and robust activation in fMRI (Castelli et al., 2000, 2002; White et al., 2011)	Frith–Happe animations of social and random interactions	Medial prefrontal cortex; temporal parietal junction; inferior and superior temporal sulcus
Biological motion • Localizer: (Peuskens et al., 2005)	Point light displays of biological motion versus random motion versus static dot displays	MT+; visual cortex
Motor strip mapping • Localizer: (Bizzi et al., 2008; Morioka et al., 1995)	Right versus left toe movements or finger movements; tongue movements	Motor and somatosensory cortex
Higher order relational processing • Localizer: (Smith et al., 2007)	Alternating blocks of judgments about relations among features versus feature matching	Anterior prefrontal cortex

Please cite this article as: Barch, D.M., et al., Function in the human connectome: Task-fMRI and individual differences in behavior, NeuroImage (2013), http://dx.doi.org/10.1016/j.neuroimage.2013.05.033

Table 2
NIH Toolbox measures included in the HCP.

Domain	Subdomain (measure name)
Cognition	Episodic memory (Picture Sequence Memory)
	Executive function/cognitive flexibility (Dimensional Change Card Sort)
	Executive function/inhibition (Flanker Task)
	Language/vocabulary comprehension (Picture Vocabulary)
	Processing speed (Pattern Completion Processing Speed)
	Working memory (List Sorting)
	Language/reading decoding (Oral Reading Recognition)
Emotion[a]	Negative affect (Sadness, Fear, Anger)
	Psychological well-being (Positive Affect, Life Satisfaction, Meaning and Purpose)
	Social relationships (Social Support, Companionship, Social Distress, Positive Social Development)
	Stress and self efficacy (Perceived Stress, Self-Efficacy)
Motor	Dexterity (9-hole Pegboard)
	Endurance (2 min walk test)
	Locomotion (4-meter walk test)
	Strength (Grip Strength Dynamometry)
Sensory	Audition (Words in Noise)
	Olfaction (Odor Identification Test)
	Taste (Taste Intensity Test)
	Pain (Pain Intensity and Interference Surveys)

[a] All emotion measures and the pain measures are self-report.

In our design of the tfMRI battery, our goal was to be as efficient as possible, so as to include the maximum number of tasks possible within an amount of time feasible given subject burden concerns. More specifically, this goal involved three types of design choices. First, where possible, we opted to use block design paradigms rather than event-related paradigms, given their enhanced efficiency (Liu et al., 2001). Although we recognized that event-related designs can afford more sophisticated analyses in many cases, we felt that the efficiency benefits of blocked designs were more important for this specific project. One consideration in making this decision was that because HCP data will be publically available, investigators can use block-design HCP findings as a springboard for future investigations using more granular task variants and modeling approaches. At the same time, there were some tasks for which we were concerned that a blocked design would alter the psychological process of interest to the point of invalidating the paradigm. For such tasks (dorsal and ventral attention systems, gambling), our piloting included an explicit comparison of blocked and event-related versions. Second, where possible, we built in multiple types of contrasts within a task to allow us to address different processes and different brain systems within one task. For example, as described in the methods, the working memory task (an N-back task with 2- and 0-back load levels) was conducted with multiple stimulus types. One can ignore stimulus type and focus on only memory load comparisons to identify dorsal–frontal and parietal regions involved in working memory and cognitive control. Alternatively, one can collapse across memory load and focus only on stimulus type comparisons to identify temporal, occipital and parietal regions that respond to specific stimulus types. Third, if our pilot analyses suggested that activation of a set of brain regions associated with a specific function could be identified within the context of another task, we did not include a separate task to isolate those regions. For example, our piloting included a task using point-light walkers (Antal et al., 2008) to assess regions associated with biological motion. However, our phase I results revealed that these same brain regions were also activated in the social cognition task that involved objects moving in biologically plausible ways. Thus, our final battery did not include a separate biological motion task.

The discussion above provides our logic and rationale for the design of the behavior and individual difference batteries as well as the TFMRI. Below we provide specific details about each of the tasks and measures, describe the results of the initial Phase I piloting, and provide preliminary data on the patterns of activation associated with each of the fMRI tasks, at both group and individual levels, during the ongoing Phase II data collection.

Methods

Overview

We conducted several pilot studies during Phase I of the HCP, prior to the start of the main data collection in Phase II. In the main text of this manuscript, we present data from Phase II so as to familiarize readers with the exact protocol that will be applied in the full sample of 1200 individuals. We present data from the Phase I pilot studies that informed our decisions as to what to include in Phase II in the Supplemental materials and refer to it where appropriate.

Participants

We present behavioral data from the 77 participants whose data will be part of the first quarter data release of Phase II. We also present imaging data from 20 of these participants who are unrelated to each other. For a complete description of our inclusion and exclusion criteria, please see Van Essen et al. (2012, in press) for additional details. Briefly, all the participants are between the ages of 22 and 35, with no previously documented history of psychiatric, neurological, or medical disorders known to influence brain function. Of the 77 participants included in the report of the behavioral data, 58 are female and 19 are male, 3 are between the ages of 22–25, 27 are between the ages of 26–30 and 47 are between the ages of 31–35 (see Van Essen et al. (in press) for reasons for reporting ages this way). Of the 20 participants whose imaging data is included in the current report, 12 are female, 1 is between the ages of 22–25, 5 are between the ages of 26–30 and 14 are between the ages of 31–35.

Table 3
Additional behavioral and individual difference measures including in the HCP.

Domain	Subdomain (measure name)
Visual processing	Visual acuity (Electronic Visual Acuity System)
	Color vision (Farnsworth Test)
	Contrast sensitivity (Mars Contrast Sensitivity)
Personality	Five factor model (NEO-FFI)
Cognition	Self-regulation/impulsivity (Delay Discounting)
	Sustained attention (Short Penn Continuous Performance Test)
	Verbal episodic memory (Penn Word Memory Test)
	Spatial orientation (Variable Short Penn Line Orientation Test)
	Fluid intelligence (Penn Progressive Matrices)
Emotion	Emotion recognition (Penn Emotion Recognition Test)
Psychiatric, substance abuse, and life function	Life function (Achenbach Adult Self-Report)
	Psychiatric clinical symptoms (Semi-Structured Assessment for the Genetics of Alcoholism)
	Nicotine dependence (Fagerstrom Test for Nicotine Dependence)
	Current substance use (Breathalyzer, Urine Drug Screen, Self-Report)
Physical function	Hematocrit levels
	Menstrual cycle and hormonal status
	Thyroid function (Thyroid Stimulating Hormone Levels)
	Glucose function (Hemoglobin A1c)
Other	Cognitive status (Mini Mental Status Exam)
	Sleep (Pittsburgh Sleep Questionnaire)

Please cite this article as: Barch, D.M., et al., Function in the human connectome: Task-fMRI and individual differences in behavior, NeuroImage (2013), http://dx.doi.org/10.1016/j.neuroimage.2013.05.033

Behavioral and individual difference paradigms

NIH Toolbox behavioral measures

The Toolbox measures (see http://www.nihtoolbox.org for full development history) are either fully computer-administered and scored using algorithms embedded in the software, or tester-administered with the results input through a standard interface into the same database. The HCP is using the majority of the Toolbox measures (see Table 2), but is not using any Toolshed measures. The HCP is not using the visual acuity measure from the Toolbox because it requires a larger testing space than was available (see below for alternative measure included in the HCP) and is not using the balance measure. The HCP staff underwent extensive training with the Toolbox staff prior to the launch of Phase II. For the majority of the participants, all of the NIH Toolbox measures will be administered in the same behavioral session, lasting approximately 1.5 h.

Non-Toolbox behavioral measures

We felt that there were several additional domains of behavior and individual differences not covered by the NIH Toolbox that would be important to assess. Thus, we also collect the following measures in an additional behavioral session that lasts approximately 1.5 to 2 h. This battery is implemented in a web-based platform developed by the Gur laboratory at the University of Pennsylvania (Gur et al., 2001b, 2010), and uses some of the measures that their group has developed. Here we describe the additional tests being administered (see Table 3), and full details on the task parameters can be found in the Supplemental materials.

Visual processing. The HCP is assessing three different components of visual processing, using; 1) the Electronic Visual Acuity (EVA) system running the Electronic Early Treatment of Diabetic Retinopathy (E-ETDR) protocol (Beck et al., 2003; Moke et al., 2001) to assess visual acuity; 2) the Farnsworth Test to assess *color vision* — a valid and reliable measure that provides more quantitative information than the commonly used Ishihara Test (Cole, 2007); and 3) the Mars Contrast Sensitivity Test (Arditi, 2005), to assess *contrast sensitivity* — a brief, valid and reliable measure that improves upon the traditional Pelli–Robson measure (Dougherty et al., 2005; Haymes et al., 2006; Thayaparan et al., 2007).

Self-regulation. We are measuring self-regulation using a delay discounting paradigm that captures the undervaluing of rewards that are delayed in time. We use a version of the discounting task that identifies 'indifference points' at which a person is equally likely to choose a smaller reward (e.g., $100) sooner versus a larger reward later (e.g., $200 in 3 years). Based on the work of Green and Myerson (Estle et al., 2006; Green et al., 2007), we use an adjusting-amount approach, in which delays are fixed and reward amounts are adjusted on a trial-by-trial basis based on participants' choices, to rapidly hone in on indifference points. This approach has been repeatedly validated to provide reliable estimates of delay discounting (Estle et al., 2006). As a summary measure, we use an area-under-the-curve discounting measure (AUC) that provides a valid and reliable index of how steeply individual discounts delayed rewards (Myerson et al., 2001), with both one measure for a high monetary amount ($40,000) and one for a smaller monetary amount ($200). Q6

Sustained attention. We measure continuous *sustained attention* using the Short Penn Continuous Performance Test (Number/Letter Version) (Gur et al., 2001a, 2001b, 2010).

Verbal memory. To complement the NIH Toolbox measure non-verbal episodic memory, we are assessing verbal episodic memory using Form A of the Penn Word Memory Test (Gur et al., 2001b, 2010).

Visual–spatial processing. The NIH Toolbox does not contain any measures of visual–spatial processing. Thus, we are measuring spatial orientation processing using the Variable Short Penn Line Orientation Test (Gur et al., 2001b, 2010).

Emotion processing. The NIH Toolbox contains only self-report measures of emotional function. Thus, to obtain a behavioral measure of emotion processing, we are using the Penn Emotion Recognition Test (Gur et al., 2001b, 2010).

Fluid intelligence. Although the Toolbox contains measures of crystallized IQ (e.g., vocabulary acquisition), an aspect of IQ strongly influenced by educational opportunities, and measures of executive function (which are both theoretically and empirically related to fluid intelligence), it does not contain a specific measure of fluid intelligence. This construct is strongly linked to specific functional outcomes and to variations in neuronal structure and function in humans (Duncan, 2003, 2005; Duncan et al., 2000). The most commonly used measure of fluid intelligence is Raven's Progressive Matrices (Christoff et al., 2001; Conway et al., 2005; Gray et al., 2003, 2005; Prabhakaran et al., 1997; Wendelken et al., 2008). We use Form A of

Table 4
Parameters for HCP Phase II task-fMRI.

Parameter	fMRI session 1			fMRI session 2			
Task	Working memory	Gambling	Motor	Language	Social cognition	Relational processing	Emotion processing
Frames per run	405	253	284	316	274	232	176
Run duration (min)	5:01	3:12	3:34	3:57	3:27	2:56	2:16
# of task blocks/run	8 (1/2 0-back, 1/2 2-back)	4 (1/2 reward, 1/2 punish)	10 (2 of each body part)	8 (1/2 story, 1/2 math)	5 (1/2 TOM, 1/2 Random)[b]	6 (1/2 relational, 1/2 control)	6 (1/2 face, 1/2 shape)
Duration of task blocks (s)[a]	25	28	12	See text	23	16	18
# of trials/block	10	8	10	See text	1	4 relational, 5 control	6
Duration of trial (s)	2.5	3.5	1.2	See text	20 (movie), 3 response	4 relational, 3.2 control	3
# of fixation blocks/run	4	4	3	NA	5	3	0
Duration of fixation blocks (s)	15	15	15	NA	15	16	NA
Task cue at start of block	Yes	No	Yes	No	No	No	Yes
Duration of task cue (s)	2.5	NA	3	NA	NA	NA	3
Duration of task initiation countdown at start of run (s)	8	8	8	NA	8	8	8

[a] Duration of task block does not include duration of task cue at start of block if one is present.
[b] Run 1 contains 2 Social and 3 Random motion blocks and Run 2 contains 3 Social and 2 Random motion blocks.

Please cite this article as: Barch, D.M., et al., Function in the human connectome: Task-fMRI and individual differences in behavior, NeuroImage (2013), http://dx.doi.org/10.1016/j.neuroimage.2013.05.033

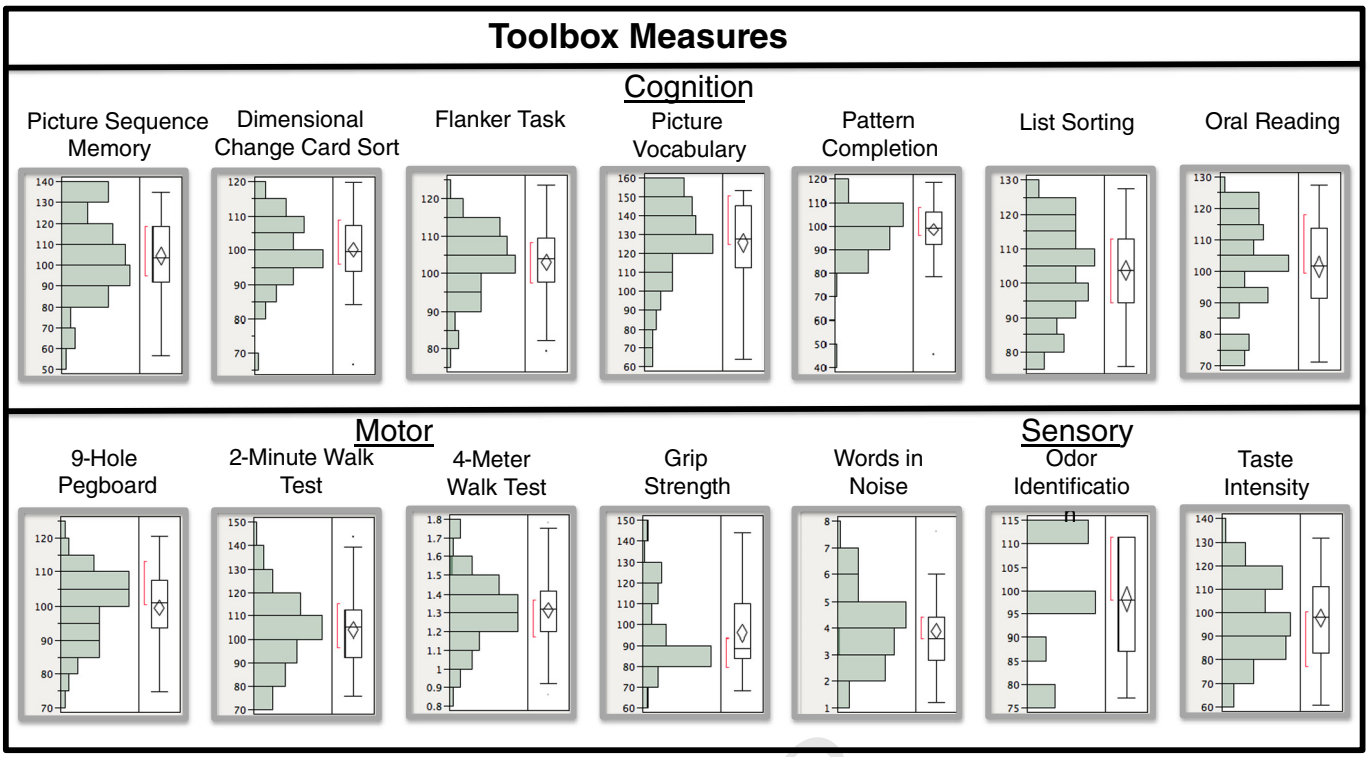

Fig. 1. Distribution of scores for NIH Toolbox measures. Boxplots showing the data from the 77 participants that constitute the first quarterly release of data for the Human Connectome Project. The ends of the box represent the 25th and 75th quantiles. The vertical line within the box represents the median value, and the diamond within the box illustrates the mean and the upper and lower 95% confidence intervals around the mean. The lines extending from the box are called whiskers and represented 1.5× the interquartile range (the difference between the first and the third quartiles) in either direction. The red bracket next the box illustrates the densest 50% of the observations (called the shortest half).

an abbreviated version of the Raven's developed by Gur and colleagues (Bilker et al., 2012).

Additional individual difference measures

Personality and function. There is consensus that a five factor model captures the major facets of human personality across cultures (Heine and Buchtel, 2009): a) neuroticism; b) extroversion/introversion; c) agreeableness; d) openness; and e) conscientiousness (Goldberg, 1993; McCrae and Costa, 2008). We are administering the 60 item version of the Costa and McRae Neuroticism/Extroversion/Openness Five Factor Inventory (NEO-FFI) (McCrae and Costa, 2004), which has shown excellent reliability and validity (McCrae and Costa, 2004). The NIH Toolbox contains self-report measures of a number of important domains of experience (e.g., stress, social relationships and positive and negative affectivity). To obtain additional self-report information on an even broader variety of domains, we also administer the Achenbach Adult Self-Report (ASR) for ages 18–59 (Achenbach, 2009). Specifically, we administer the 123 items from Section VIII of this instrument. These can be used to generate the ASR Syndrome Scales and the ASR DSM-Oriented Scales.

Psychiatric, neurological and substance use assessments. As part of the screening and assessment process, all the participants are given a comprehensive assessment of psychiatric and substance use history over the phone, using the Semi-Structured Assessment for the Genetics of Alcoholism (SSAGA) (Bucholz et al., 1994). The SSAGA is a well-validated diagnostic instrument used in numerous previous large scale studies (Bucholz et al., 1994; Hesselbrock et al., 1999). It assesses a range of diagnostic categories (substance, mood, anxiety, eating disorders and adult ADHD), as well as antisocial personality disorder, using both DSM-IV criteria and either RDC criteria or ICD criteria, and provides information about both current and lifetime experiences. This instrument also contains the Fagerstrom Test for Nicotine Dependence (Heatherton et al., 1991; Kozlowski et al., 1994). The participants are given a brief assessment of parental history of psychiatric and neurological disorders (yes/no for schizophrenia or psychosis, depression, bipolar, anxiety that needed treatment, drug or alcohol problems, Alzheimer's Disease or dementia, Parkinson's disease, or Tourette's

Table 5
Distribution of scores for emotion self report measures from the NIH Toolbox.

	Mean	Median	Minimum	Maximum	Standard deviation
Negative affect					
Sadness	44.7	44.7	26.5	75.2	11.1
Fear — affect	47.2	47.3	24.9	69.5	9.0
Fear — somatic arousal	48.8	50.7	28.7	74.3	10.7
Anger — affect	47.2	46.3	26.2	69.2	10.6
Anger — hostility	49.4	49.2	27.3	70.2	8.5
Anger — physical aggression	46.8	38.9	31.6	71.5	11.0
Psychological well-being					
Positive affect	48.6	51.0	23.6	66.4	9.4
General life satisfaction	52.8	53.8	23.1	79.1	11.2
Meaning and purpose	49.5	48.8	29.2	74.4	10.1
Social relationships					
Emotional support	48.8	50.9	27.3	59.3	8.6
Instrumental support	47.1	46.8	30.5	66.5	8.1
Friendship	49.4	49.9	24.1	66.5	9.8
Loneliness	49.9	48.9	35.2	72.3	9.6
Perceived hostility	50.1	48.6	35.5	71.4	10.0
Perceived rejection	49.6	48.8	35.6	73.7	8.6
Stress and self-efficacy					
Perceived stress	47.9	46.9	33.4	78.9	9.5
Self-efficacy	48.6	48.9	22.4	64.9	7.5
Pain interference	46.0	44.1	38.6	71.6	8.2

Please cite this article as: Barch, D.M., et al., Function in the human connectome: Task-fMRI and individual differences in behavior, NeuroImage (2013), http://dx.doi.org/10.1016/j.neuroimage.2013.05.033

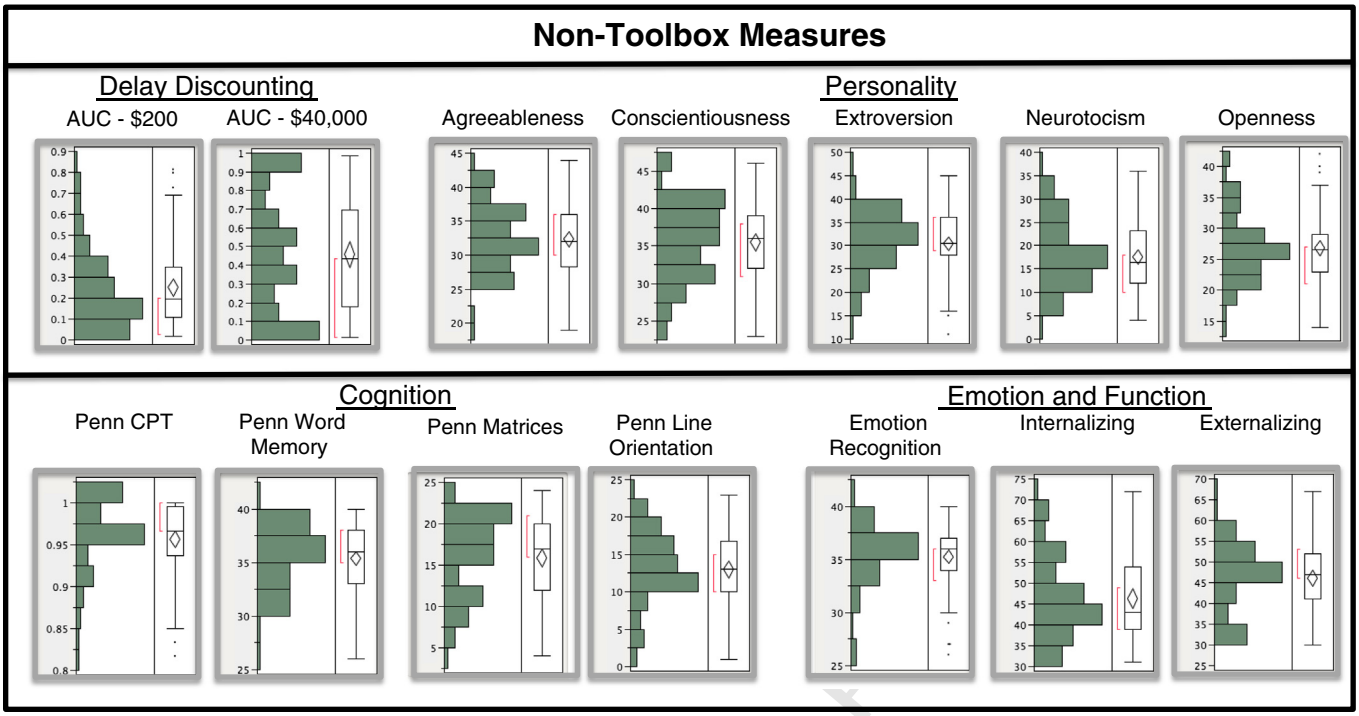

Fig. 2. Distribution of scores for non-Toolbox measures. See Fig. 1 caption.

syndrome). The participants are also given a breathalyzer and a urine drug screen (cocaine, THC, opiates, amphetamine, methamphetamine, oxycontin) on each day of testing. These drug screens were not used as an exclusion, but rather for characterization. In addition, on the last day of testing, the participants fill out a seven day retrospective report of alcohol and tobacco use.

Menstrual cycle, hormones, sleep, and cognitive status. Female participants are asked questions about their hormonal status and menstrual cycle during the intake interview at their first in person session. In addition, the participants are administered the Pittsburgh Sleep Questionnaire (Buysse et al., 1989) as a measure of sleep quality and the Mini Mental Status Exam (Folstein et al., 1975) as a broad measure of cognitive status (the participants are excluded if they score below 27) (Crum et al., 1993).

Handedness. Handedness is assessed using the Edinburgh Handedness questionnaire (Oldfield, 1971).

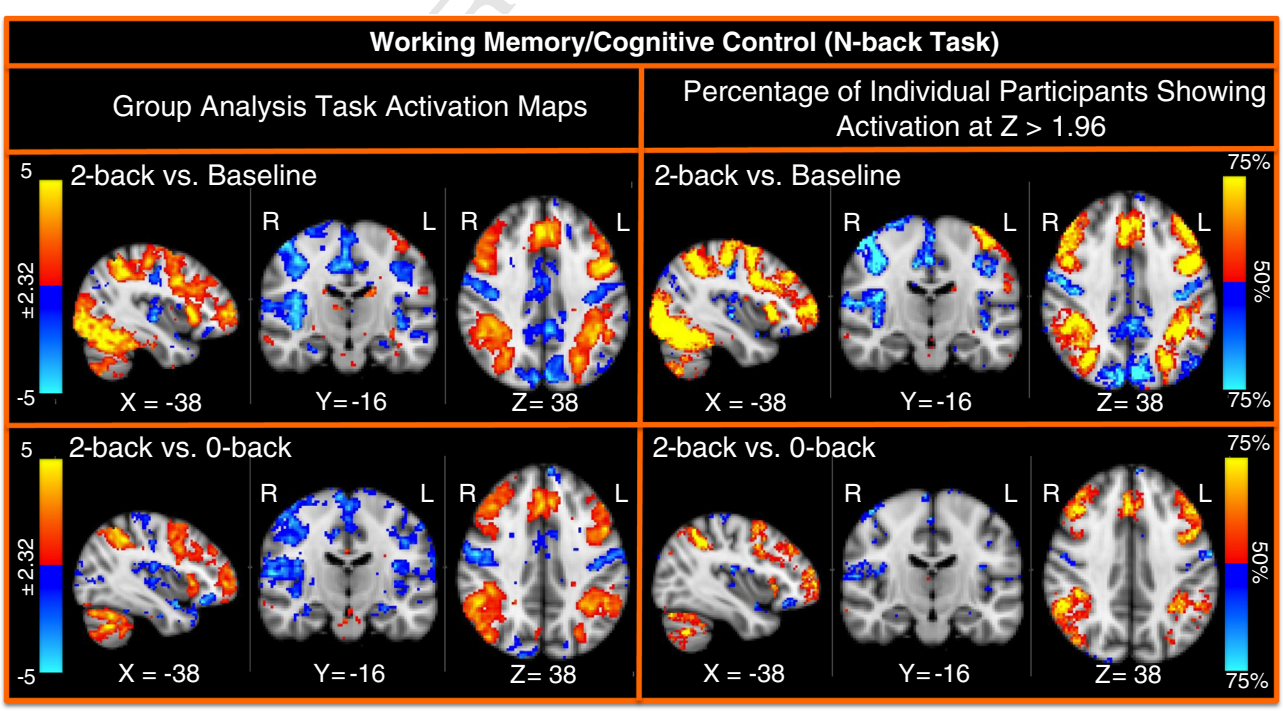

Fig. 3. Group and activation count maps for the working memory task.

Please cite this article as: Barch, D.M., et al., Function in the human connectome: Task-fMRI and individual differences in behavior, NeuroImage (2013), http://dx.doi.org/10.1016/j.neuroimage.2013.05.033

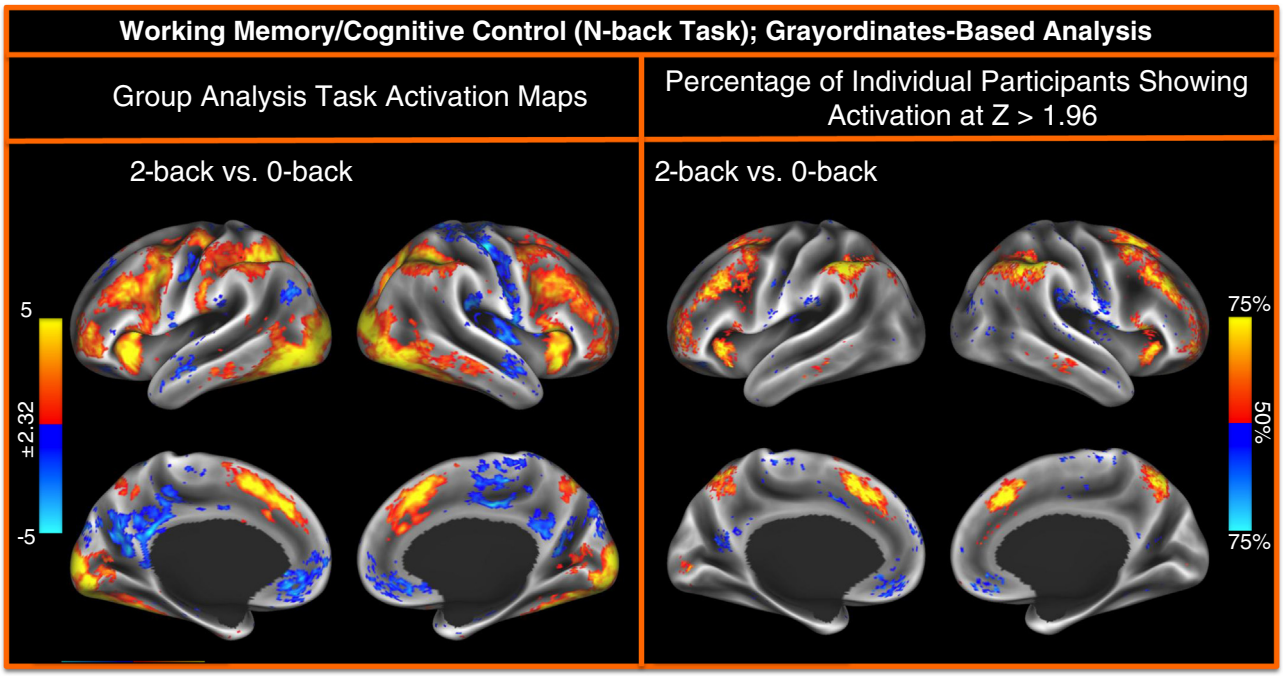

Fig. 4. Group and activation count maps for the working memory task from the grayordinates-based analysis.

Physical function. We also assess blood pressure, height and weight, hematocrit levels to assess the volume percentage of red blood cells in the blood, Thyroid Stimulating Hormone as an endocrine measure, and Hemoglobin A1c as a measure of glucose levels over time.

tfMRI paradigms

Overview. We considered a number of different domains when developing the battery for the tfMRI component of the HCP (see Table 1). We initially considered including retinotopy, and began to pilot two versions of retinotopic mapping (phase encoding and an event-related version). It rapidly became clear that we would not be able to obtain a reliable and informative assessment of retinotopy in the available amount of in-scanner time per participant, especially considering that we do not expect tremendous individual differences. Development of an efficient retinotopy paradigm is still under consideration for the paradigms to be administered on the 7T at the University of Minnesota on a subset of participants. The first pilot study had the participants complete the following tasks across two baseline sessions, and then return to complete the same tasks again two weeks later (using different stimuli where possible): working memory, recognition memory, emotional processing (both the IAPS and Hariri task), language (sentence judgment), biological motion, social cognition, dorsal and ventral attention systems (both a blocked and an event-related version), gambling (both a blocked and an event-related version), and the motor mapping task. The second pilot study compared a different version of a language task (story versus math) to the sentence processing task, and also included a relational processing task designed to activate the anterior prefrontal cortex. Description of the other tasks that were piloted in Phase I are provided in the Supplemental materials (i.e., dorsal and ventral attention, sentence processing, biological motion, negative IAPS image processing, event-related gambling task). Below we describe the tasks that we are using in Phase II. For each task, the participants are provided with instructions outside of the scanner. They are then given a very brief reminder of the task and a refresher on the button box mappings just before the start of each task.

Working memory/category specific representations. We chose to use a version of the N-back task to assess working memory/cognitive control because: 1) there was data suggesting that it could be used as a functional localizer: (Drobyshevsky et al., 2006); 2) there was evidence suggesting that associated brain activations were reliable across subjects (Drobyshevsky et al., 2006) and time (Caceres et al., 2009); and 3) we could design the task so as to allow us to assess multiple embedded contrasts (e.g., memory load, stimulus type, error related activity, conflict related activity). The specifics of the N-back task as it is being run in Phase II are shown in Table 4. As described in the Introduction, to maximize efficiency, we embedded the category specific representations component within the working memory task, by presenting blocks of trials that consisted of pictures of faces, places, tools and body parts. Within each run, the 4 different stimulus types are presented in separate blocks within the run. Within each run, 1/2 of the blocks use a 2-back working memory task (respond 'target' whenever the current stimulus is the same as the one two back) and 1/2 use a 0-back working memory task (a target cue is presented at the start of each block, and the person must respond 'target' to any presentation of that stimulus during the block). A 2.5 s cue indicates the task type (and target for 0-back) at the start of the block. Each of the two runs contains 8 task blocks (10 trials of 2.5 s each, for 25 s) and 4 fixation blocks (15 s each). On each trial, the stimulus is presented for 2 s, followed by a 500 ms ITI. Each block contains 10 trials, of which 2 are targets, and 2–3 are non-target lures (e.g., repeated items in the wrong n-back position, either 1-back or 3-back). The inclusion of lures is critical to ensure that the participants are using an active memory approach to the task and allows one to assess conflict related activity as well as error related activity.

We chose faces, places, tools and body parts as the four categories of stimuli because of evidence that these stimuli reliably engage distinct cortical regions (Downing et al., 2001; Fox et al., 2009; Peelen and Downing, 2005; Taylor et al., 2007) and because the associated brain activations are reliable across subjects (Downing et al., 2001; Fox et al., 2009) and time (Kung et al., 2007; Peelen and Downing, 2005). The stimuli were obtained from a number of previous studies

Please cite this article as: Barch, D.M., et al., Function in the human connectome: Task-fMRI and individual differences in behavior, NeuroImage (2013), http://dx.doi.org/10.1016/j.neuroimage.2013.05.033

using face (Pinsk et al., 2009), place (Kanwisher, 2001; O'Craven and Kanwisher, 2000; Park and Chun, 2009), body parts (Bracci et al., 2010; Downing et al., 2001, 2006b; Peelen and Downing, 2005; Pinsk et al., 2009; Saxe et al., 2006) and tool (Downing et al., 2006a; Peelen and Downing, 2005; Wierenga et al., 2009) stimuli.

Recognition memory. After the participants exit the scanner from the session that includes the Working Memory tasks, they are given a "Remember, Know, New" item recognition test for the faces and places presented during the working memory task, as well as an equal number of new faces and places similar on visual characteristics (e.g., an equal number of old and new stimuli came from the same stimuli sets). We did not include body parts or tools as we did not have a sufficient number of unique stimuli to serve as "new" items. Responses to this recognition memory test can be used to segregate events to analyze the working memory trials as a function of whether the item was subsequently recognized (remember or know) or not (new), which is referred to as a subsequent memory analysis. Each item is presented for 2 s. There is then a 2 s ITI before the next stimulus. There are 48 old and 48 new stimuli (1/2 of each stimulus type). Please see the Supplemental materials for exact instructions. Data from this subsequent memory analysis will be presented in a future publication.

Incentive processing. This task was adapted from the one developed by Delgado et al. (2000), and was chosen based on prior evidence that the task elicits activations in the striatum and other reward related regions that are robust and reliable across the subjects (Delgado et al., 2000; Forbes et al., 2009; May et al., 2004; Tricomi et al., 2004). The participants play a card guessing game where they are asked to guess the number on a mystery card (represented by a "?") in order to win or lose money. They are told that potential card numbers range from 1 to 9 and to indicate if they think the mystery card number is more or less than 5 by pressing one of two buttons on the response box. Feedback is the number on the card (generated by the program as a function of whether the trial was a reward, loss or neutral trial) and either: 1) a green up arrow with "$1" for reward trials, 2) a red down arrow next to −$0.50 for loss trials; or 3) the number 5 and a gray double headed arrow for neutral trials. The "?" is presented for up to 1.5 s (if the participant responds before 1.5 s, a fixation cross is displayed for the remaining time), following by feedback for 1.0 s. There is a 1.0 s ITI with a "+" presented on the screen. The task is presented in blocks of 8 trials that are either mostly reward (6 reward trials pseudo randomly interleaved with either 1 neutral and 1 loss trial, 2 neutral trials, or 2 loss trials) or mostly loss (6 loss trials interleaved with either 1 neutral and 1 reward trial, 2 neutral trials, or 2 reward trials). In each of the two runs, there are 2 mostly reward and 2 mostly loss blocks, interleaved with 4 fixation blocks (15 s each). All the participants are provided with money as a result of completing the task, though it is a standard amount across subjects.

Motor. This task was adapted from the one developed by Buckner and colleagues which had evidence that it could identify effector specific activations in individual subjects (Buckner et al., 2011; Yeo et al., 2011). The participants are presented with visual cues that ask them to tap their left or right fingers, squeeze their left or right toes, or move their tongue to map motor areas. Each block of a movement type lasts 12 s (10 movements), and is preceded by a 3 s cue. In each of the two runs, there are 13 blocks, with 2 of tongue movements, 4 of hand movements (2 right and 2 left), 4 of foot movements (2 right and 2 left) and three 15 s fixation blocks per run.

Language processing. The task being used in Phase II was developed by Binder et al. (2011) and used the E-prime scripts kindly provided by these investigators, which were then modified for our purposes. The task consists of two runs each interleaved by 4 blocks of a story task and 4 blocks of a math task. As described in detail in Binder et al. Q7

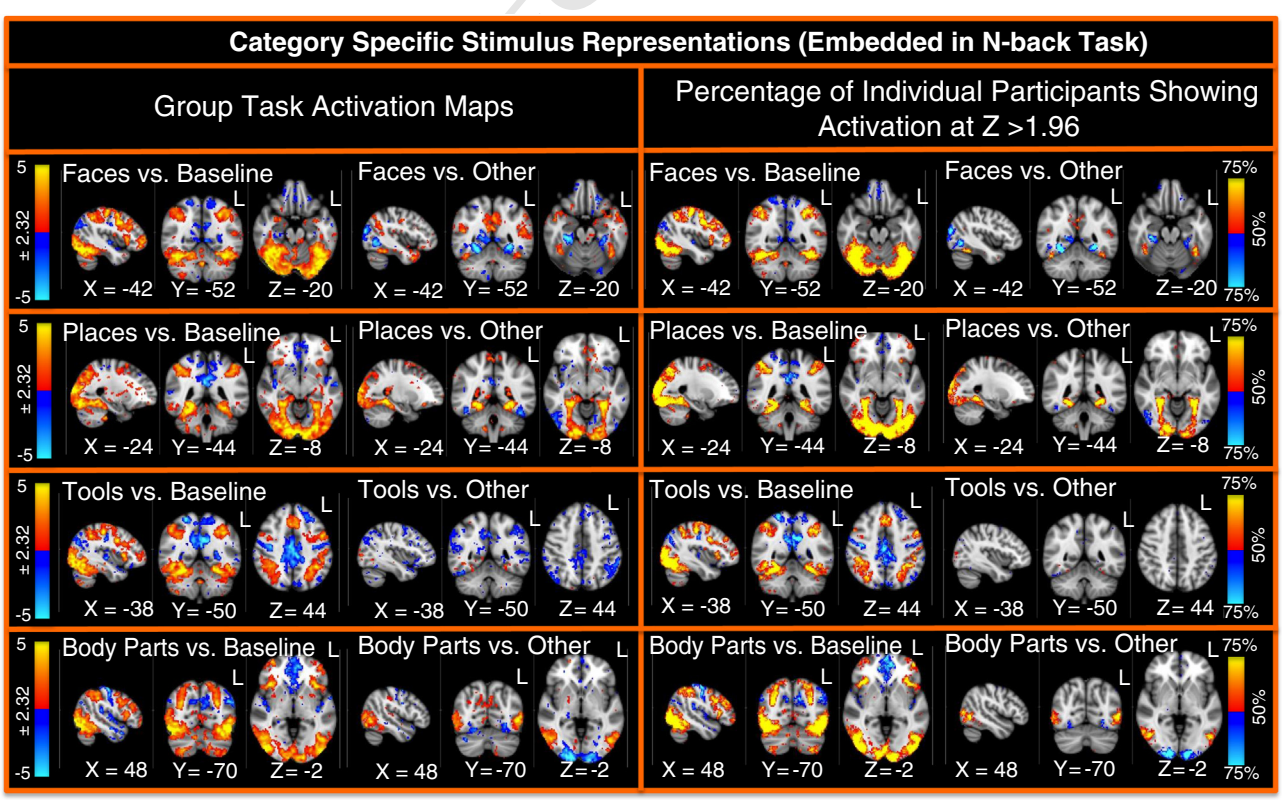

Fig. 5. Group and activation count maps for the category specific representation contrasts.

Please cite this article as: Barch, D.M., et al., Function in the human connectome: Task-fMRI and individual differences in behavior, NeuroImage (2013), http://dx.doi.org/10.1016/j.neuroimage.2013.05.033

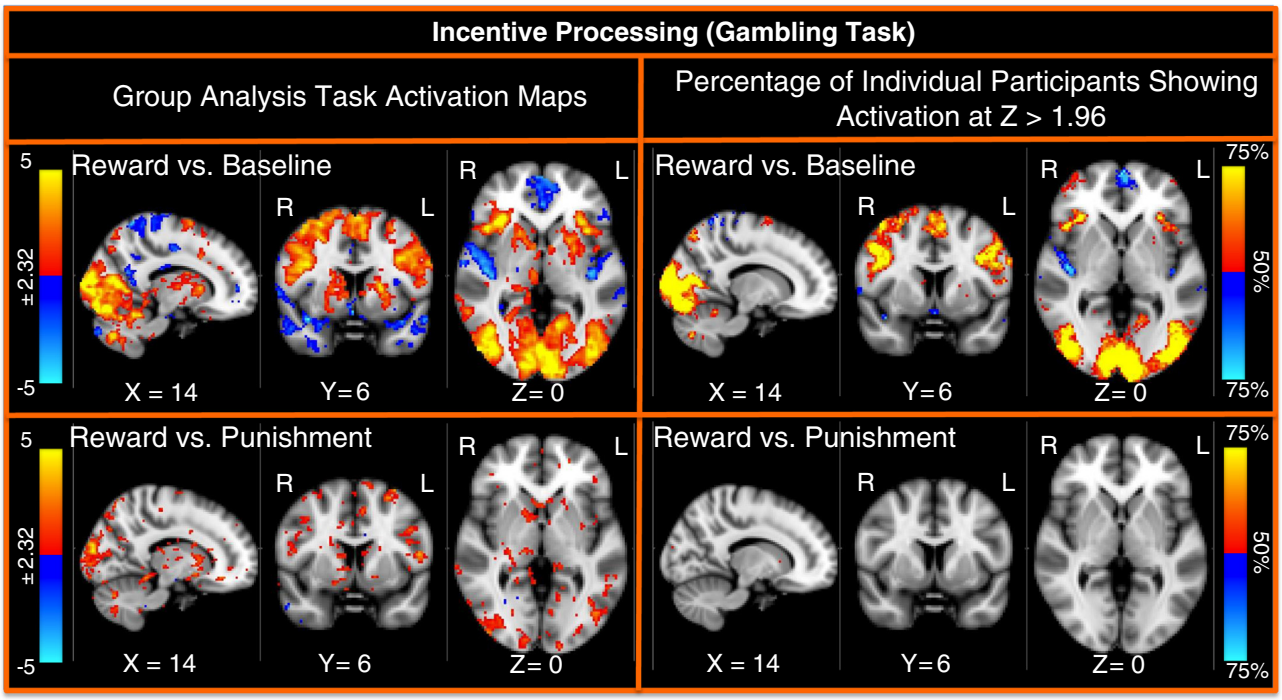

Fig. 6. Group and activation count maps for the incentive processing task.

(2011), the goal of including the math blocks was to provide a comparison task that was attentionally demanding, similar in auditory and phonological input, and unlikely to generate activation of anterior temporal lobe regions involved in semantic processing, though likely to engage numerosity related processing in the parietal cortex. The lengths of the blocks vary (average of approximately 30 s), but the task was designed so that the math task blocks match the length of the story task blocks, with some additional math trials at the end of the task to complete the 3.8 min run as needed. The story blocks present participants with brief auditory stories (5–9 sentences) adapted from Aesop's fables, followed by a 2-alternative forced-choice question that asks the participants about the topic of the story. The example provided in the original Binder paper (p. 1466) is "*For example, after a story about an eagle that saves a man who had done him a favor, participants were asked, 'That was about revenge or reciprocity?'*" The math task also presents trials auditorily and requires the subjects to complete addition and subtraction problems. The trials present the subjects with a series of arithmetic operations (e.g., "Fourteen plus twelve"), followed by "equals" and then two choices (e.g., "twenty-nine or twenty-six"). The participants push a button to select either the first or the second answer. The math task is adaptive to maintain a similar level of difficulty across the participants. For more details on the task, see Binder et al. (2011).

Social cognition (theory of mind). An engaging and validated video task was chosen as a measure of social cognition, given evidence that it generates robust task related activation in brain regions associated with social cognition and is reliable across subjects (Castelli et al., 2000, 2002; Wheatley et al., 2007; White et al., 2011). The participants are presented with short video clips (20 s) of objects (squares, circles, triangles) either interacting in some way, or moving randomly. These videos were developed by either Castelli et al. (2000) or Wheatley et al. (2007). After each video clip, the participants chose between 3 possibilities: whether the objects had a social interaction (an interaction that appears as if the shapes are taking into account each other's feelings and thoughts), Not Sure, or No interaction (i.e., there is no obvious interaction between the shapes and the movement appears in random). Each of the two task runs has 5 video blocks (2 Mental and 3 Random in one run, 3 Mental and 2 Random in the other run) and 5 fixation blocks (15 s each). Of note, the video clips were shortened to 20 s (the Castelli et al. clips were originally 40 s) by either splitting the videos in two or truncating them. We conducted a pilot study in Phase I in which the participants made ratings about the presence or absence of mental interactions in the videos to confirm that the shorter videos elicited similar responses to the longer videos.

Relational processing. This task was adapted from the one developed by Smith et al. (2007) which was demonstrated to localize activation Q8 in anterior prefrontal cortex in individual subjects. The stimuli are 6 different shapes filled with 1 of 6 different textures. In the relational processing condition, the participants are presented with 2 pairs of objects, with one pair at the top of the screen and the other pair at the bottom of the screen. They are told that they should first decide what dimension differs across the top pair of objects (shape or texture) and then they should decide whether the bottom pair of objects also differs along that same dimension (e.g., if the top pair differs in shape, does the bottom pair also differ in shape). In the control matching condition, the participants are shown two objects at the top of the screen and one object at the bottom of the screen, and a word in the middle of the screen (either "shape" or "texture"). They are told to decide whether the bottom object matches either of the top two objects on that dimension (e.g., if the word is "shape", is the bottom object the same shape as either of the top two objects). For the relational condition, the stimuli are presented for 3500 ms, with a 500 ms ITI, with four trials per block. In the matching condition, stimuli are presented for 2800 ms, with a 400 ms ITI, with 5 trials per block. Each type of block (relational or matching) lasts a total of 18 s. In each of the two runs of this task, there are 3 relational blocks, 3 matching blocks and three 16 s fixation blocks (see Table 4).

Emotion processing. This task was adapted from the one developed by Hariri and colleagues which had shown evidence as a functional localizer (Hariri et al., 2002) with moderate reliability across time

Q9 (Manuck et al., 2007). The participants are presented with blocks of trials that ask them to decide either which of two faces presented on the bottom of the screen match the face at the top of the screen, or which of two shapes presented at the bottom of the screen match the shape at the top of the screen. The faces have either angry or fearful expressions. Trials are presented in blocks of 6 trials of the same task (face or shape), with the stimulus presented for 2 s and a 1 s ITI. Each block is preceded by a 3 s task cue ("shape" or "face"), so that each block is 21 s including the cue. Each of the two runs includes 3 face blocks and 3 shape blocks. However, there was a bug in the E-prime script for this task such that the task stopped short of the last three trials of the last task block in each run. To promote comparability across the participants, we decided not to fix the bug (given that a number of subjects had already been run before it was detected) as we thought it would have minimal impact on the data. In phase I, we compared this task to one using negative and neutral IAPS pictures (see the Supplemental materials).

fMRI data acquisition

Please see Ugurbil et al. (in press) for overview of TFMRI acquisition details for Phase II. Briefly, whole-brain EPI acquisitions were acquired with a 32 channel head coil on a modified 3 T Siemens Skyra with TR = 720 ms, TE = 33.1 ms, flip angle = 52°, BW = 2290 Hz/Px, in-plane FOV = 208 × 180 mm, 72 slices, 2.0 mm isotropic voxels, with a multi-band acceleration factor of 8 (Feinberg et al., 2010; Moeller et al., 2010). Two runs of each task were acquired, one with a right-to-left and the other with a left-to-right phase encoding. Apart from run duration, therefore, the task acquisitions were identical to the resting-state fMRI acquisitions, in order to provide maximal compatibility between task and resting data.

To measure cardiac and respiratory signals, a pulse oximeter and respiratory bellows were fitted to the participants prior to the fMRI sessions. Those signals, along with the sync pulse from the scanner, were recorded by the scanner host computer at a sampling rate of 400 Hz. Physiological recording files are matched with their respective scans using a global unique identifier recorded in the DICOM files. The physiological recordings were synchronized with the onset of the first sync pulse using a custom script. These physiological measurements will be released starting at Q2. The analyses presented below do not include regressors for cardiac or respiratory signals, though future tfMRI analyses will compare GLM analyses that do versus do not account for cardiac and respiratory signals.

fMRI data processing

The HCP data analysis pipelines are primarily built using tools from FSL and FreeSurfer. The HCP "fMRIVolume" pipeline (see Glasser et al., in press, this issue) generates "minimally preprocessed" 4D time series that includes gradient unwarping, motion correction, fieldmap-based EPI distortion correction, brain-boundary-based registration of EPI to structural T1-weighted scan, non-linear (FNIRT) registration into MNI152 space, and grand-mean intensity normalization. Two approaches were used for further processing of the data. One involved volume-based smoothing and subsequent analyses using standard FSL tools. The other involved smoothing constrained to the cortical surface and subcortical gray-matter parcels and subsequent analysis using FSL tools adapted to this 'grayordinate' based approach (see Glasser et al., in press, this issue). The majority of the data presented in this paper used a volume-based fMRI processing stream, to maximize comparison to prior studies. However, we also provide examples of the grayordinate-based approach.

Volume-based analysis. For the volume-based analysis, spatial smoothing was applied using an unconstrained 3D Gaussian kernel of FWHM = 4 mm. Activity estimates were computed for the preprocessed functional time series from each run using a general linear model (GLM) implemented in FSL's FILM (FMRIB's Improved Linear Model with autocorrelation correction) (Woolrich et al., 2001). Predictors (described in more detail below) were convolved with a double gamma "canonical" hemodynamic response function (Glover, 1999) to generate the main model regressors. To compensate for slice-timing differences and variability in the HRF delay across regions, temporal derivative terms derived from each predictor were added to each GLM and were treated as confounds of no interest. Subsequently, both the 4D time series and the GLM design were temporally filtered with a Gaussian-weighted linear highpass filter with a (soft) cutoff of 200 s. Finally, the time series was prewhitened within FILM to correct for autocorrelations in the fMRI data.

Grayordinates-based analysis. The HCP has implemented a "grayordinates" based fMRI processing pipeline that allows for efficient analysis of combined cortical surface and subcortical volume representations. The grayordinates-based analysis was performed on all tasks, and two examples are shown in the results below. The grayordinates-based analysis begins with outputs of the HCP "fMRISurface" pipeline (see Glasser et al., this issue) in which the data from the cortical gray matter ribbon are projected onto the

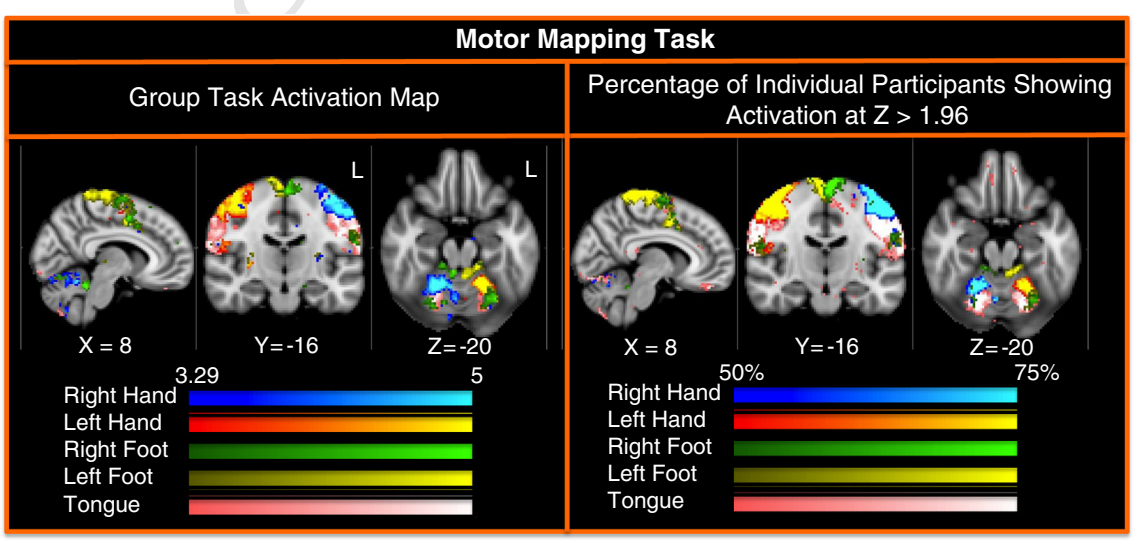

Fig. 7. Group and activation count maps for the motor mapping task.

Please cite this article as: Barch, D.M., et al., Function in the human connectome: Task-fMRI and individual differences in behavior, NeuroImage (2013), http://dx.doi.org/10.1016/j.neuroimage.2013.05.033

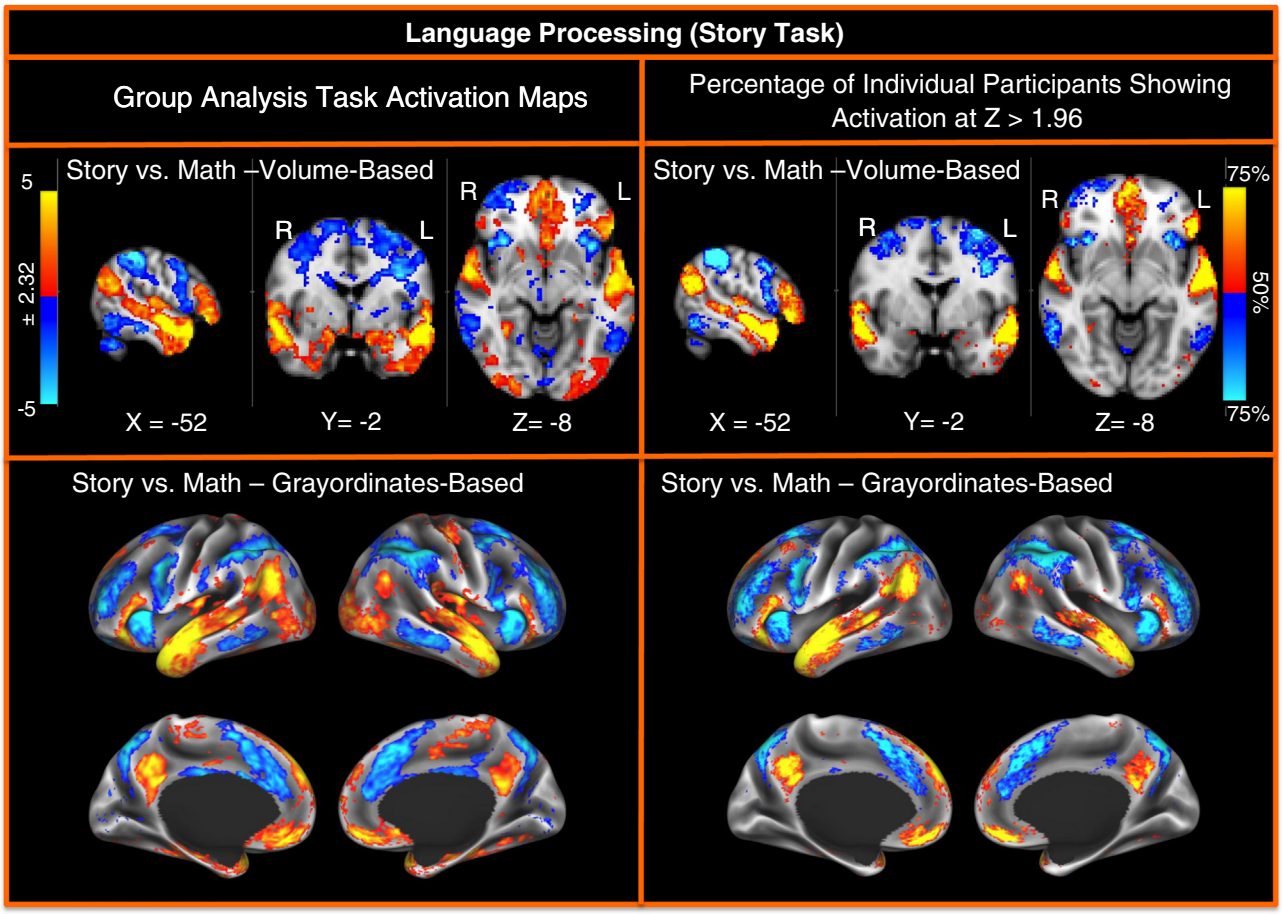

Fig. 8. Group and activation count maps for the language processing task. The upper two panels show the results from the volume-based processing stream and the bottom two panels show the results from the grayordinates-based processing stream.

surface and then onto registered surface meshes with a standard number of vertices. Subcortical data were also projected to a set of subcortical gray matter parcel voxels, and when combined with the surface data formed the standard grayordinates space (see Glasser et al., this issue). The grayordinates-based run-level analysis was carried out identically to the volume-based analysis described above aside from spatial smoothing steps, as only they are dependent on spatial neighborhood information. Smoothing of the left and right hemisphere time series and autocorrelation estimates (from FILM) were done on the surface using a geodesic Gaussian algorithm. Subcortical gray matter time series were smoothed within defined gray matter parcels. Because the surface and subcortical gray matter data in grayordinates space were already smoothed with 2 mm FWHM by the HCP fMRISurface pipeline, additional smoothing was done to bring the total smoothing to 4 mm FWHM (in 2D on the cortical surface and in 3D elsewhere) to match the volume-based analysis. The amount of additional smoothing was defined by the equation sqrt (4 mm^2 − 2 mm^2). Surface-based autocorrelation estimate smoothing was incorporated into FSL's FILM at a sigma of 5 mm. Left hemisphere surface, right hemisphere surface, and subcortical volume data from the grayordinates space were split into three NIFTI-1 matrices and processed separately for all steps. Surface outputs were converted to GIFTI at the conclusion of run-level analysis.

GLM model design. For both analysis streams, eight predictors were included in the model for *Working Memory/Category Specific Representations* — one for each type of stimulus in each of the N-back conditions (i.e., 2-Back Body, 0-Back Body, 2-Back Face and 0-Back Face). Each predictor covered the period from the onset of the cue to the offset of the final trial (27.5 s). Linear contrasts for these predictors were computed to estimate effects of interest: 2-back (vs. fixation), 0-back, 2-back vs. 0-back, each stimulus type versus baseline (e.g., Body vs. fixation, collapsing across memory load), and each stimulus type versus all others. Two predictors were included in the model for *Incentive Processing* — mostly reward and mostly loss blocks, each covering the duration of 8 trials (28 s). For this task, as with all other tasks, linear contrasts of the parameter estimates were computed to compare each condition to baseline and to each other. Five predictors were included in the *Motor* model — right hand, left hand, right foot, left foot, and tongue. Each predictor covered the duration of 10 movement trials (12 s). The 3 s cue period prior to each motor block was modeled separately to account for visual activation related to the cue word presented on the screen at the beginning of each block. Linear contrasts were computed to estimate activation for each movement type versus baseline and versus all other movement types. Two predictors were included in the *Language Processing* model — Math and Story. The Story predictor covered the variable duration of a short story, question, and response period (~30 s). The Math predictor covered the duration of a set of math questions designed to roughly match the duration of the story blocks. Two predictors were included in the *Social Cognition* model — Social and Random motion. Predictors were based on the category of the video clip rather than the rating of the individual. Each predictor covered the duration of a single video clip (20 s). Two predictors were included in the *Relational Processing* model — Relational processing and a control Matching condition. Each predictor covered the duration of 18 s composed of four trials for the Relational condition and five trials for the Matching condition. Two predictors were included in the *Emotion*

Processing model — Emotional Faces and a Shape control condition. Each predictor covered a 21 s duration composed of a cue and six trials.

Participant-level and group-level analyses. Fixed-effects analyses were conducted using FEAT to estimate the average effects across runs within-participants, and then mixed-effects analyses treating subjects as random effects were conducted using FLAME (FMRIB's Local Analysis of Mixed Effects) to estimate the average effects of interest for the group. Volume-based group-level analyses were carried out using voxel-wise comparisons in MNI space and visualized in FSLView. The grayordinates-based participant-level and group-level analyses were done identically to the volume-based analysis except that cross-run and cross-subject statistical comparisons occurred in standard grayordinates space (Glasser et al., this issue) rather than volume space. As in the individual analysis, NIFTI-1 matrices were processed separately for left and right surface and subcortical volume data, and surface outputs were converted to GIFTI at the conclusion of analysis. Participant-level and group-level z-statistic maps were combined from left and right hemisphere cortical and subcortical gray matter into the recently introduced CIFTI data format (http://www.nitrc.org/projects/cifti/; for visualization using the Connectome Workbench platform (see Marcus et al., this issue). For both analyses, group maps are displayed with a lower threshold of $z = \pm 2.32$ ($p < 0.01$, uncorrected) and an upper threshold of $z = \pm 5.00$ (Bonferroni-corrected $p < 0.066$). We present the maps at this range to allow readers to see for themselves what type of activation would be present at a threshold one might use for a focused a priori ROI ($p < 0.01$ uncorrected) or an exploratory whole brain family-wise error corrected level. All statistics are computed voxel-wise (not, for example, using cluster-based thresholding), in order to maximize simplicity of interpretation of the results.

Activation count maps. Activation count maps (ACMs) were created to demonstrate, for a particular contrast of interest, the proportion of participants that showed activation (or deactivation) at a z-threshold of 1.96 (uncorrected, two-tailed $p < 0.05$). Specifically, for each contrast of interest, a binary mask for each participant was created from voxels with z-values greater than $z = 1.96$. Subsequently, the average of the binary masks was computed across participants for each voxel, resulting in the proportion of participants with a z-value greater than 1.96 at that voxel for that particular contrast. This relatively liberal threshold was chosen because it has been demonstrated that functional localizer tasks with small amounts of data are more spatially reliable at liberal statistical thresholds (Kawabata Duncan and Devlin, 2011). In addition, a *task count map* was computed in order to demonstrate the number of tasks in which there was meaningful activation (or deactivation) for at least one contrast of interest. For each of the tasks, two maps were created such that voxels had a value of one if any contrast in that task had an ACM value greater than or equal to 70% or 50% of the participants respectively. Subsequently, the sum of those maps was computed across tasks, such that the resulting "task count map" reflected the number of tasks in which a voxel showed a z-value greater than 1.96 for at least 70% or 50% of the participants in at least one contrast. In essence, the task count map demonstrates overall spatial coverage of the tasks included in the HCP tfMRI battery.

Quality assurance metrics

The HCP developed Standard Operating Procedures that are guiding our acquisition of all aspects of HCP data, including procedures for ensuring standardization in the acquisition of all measures across research assistants and across participants. Please see Marcus et al. (this issue) for a detailed description of the quality assurance metrics being assessed for the fMRI data. Briefly, we measure both absolute and relative movement, temporal standard deviation, and smoothness. In addition, we computed SNR maps to illustrate areas of signal loss. Volume and grayordinate-based maps of temporal SNR (tSNR) were created for each run by dividing the mean signal over time of a given voxel or grayordinate by the standard deviation over time of that same voxel or grayordinate, using the data that was smoothed with a 4 mm FWHM filter. The estimate of the standard deviation was obtained from the square root of the "sigmasquareds" returned by FEAT, which is an estimate of the residual variance after whitening and model fitting. The maps were then averaged across runs and subjects for a given task.

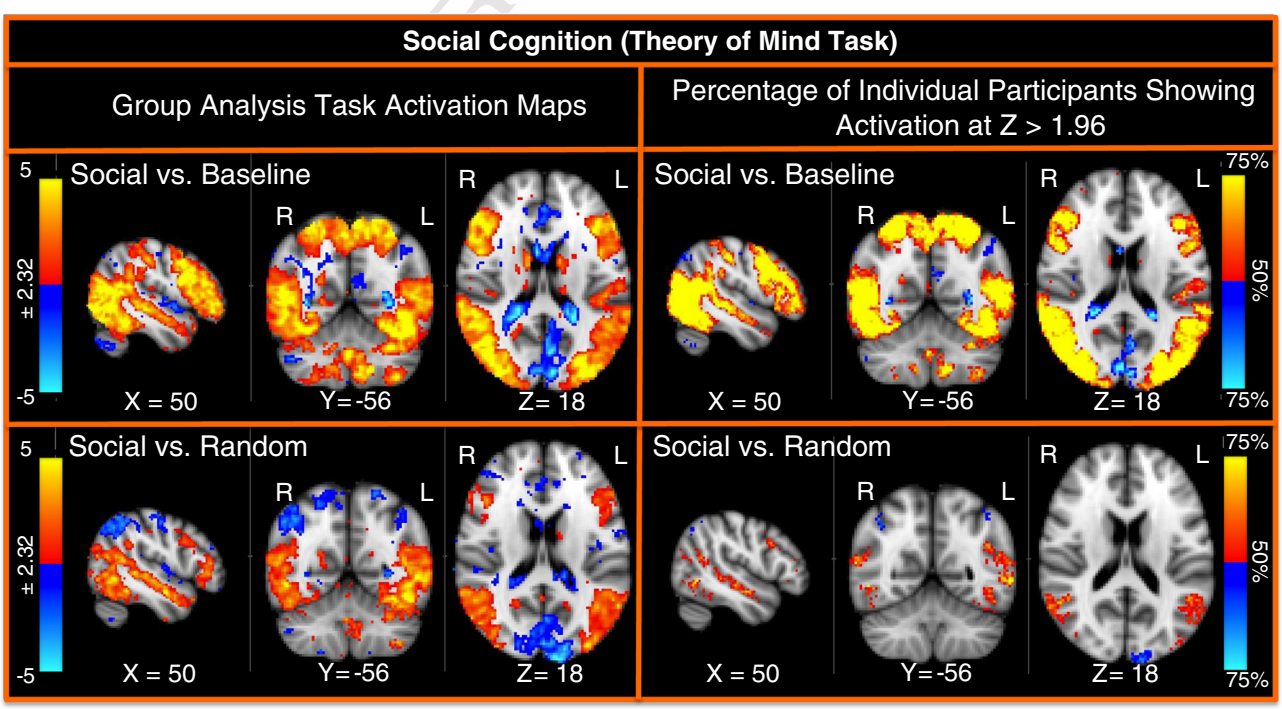

Fig. 9. Group and activation count maps for the social cognition task.

Please cite this article as: Barch, D.M., et al., Function in the human connectome: Task-fMRI and individual differences in behavior, NeuroImage (2013), http://dx.doi.org/10.1016/j.neuroimage.2013.05.033

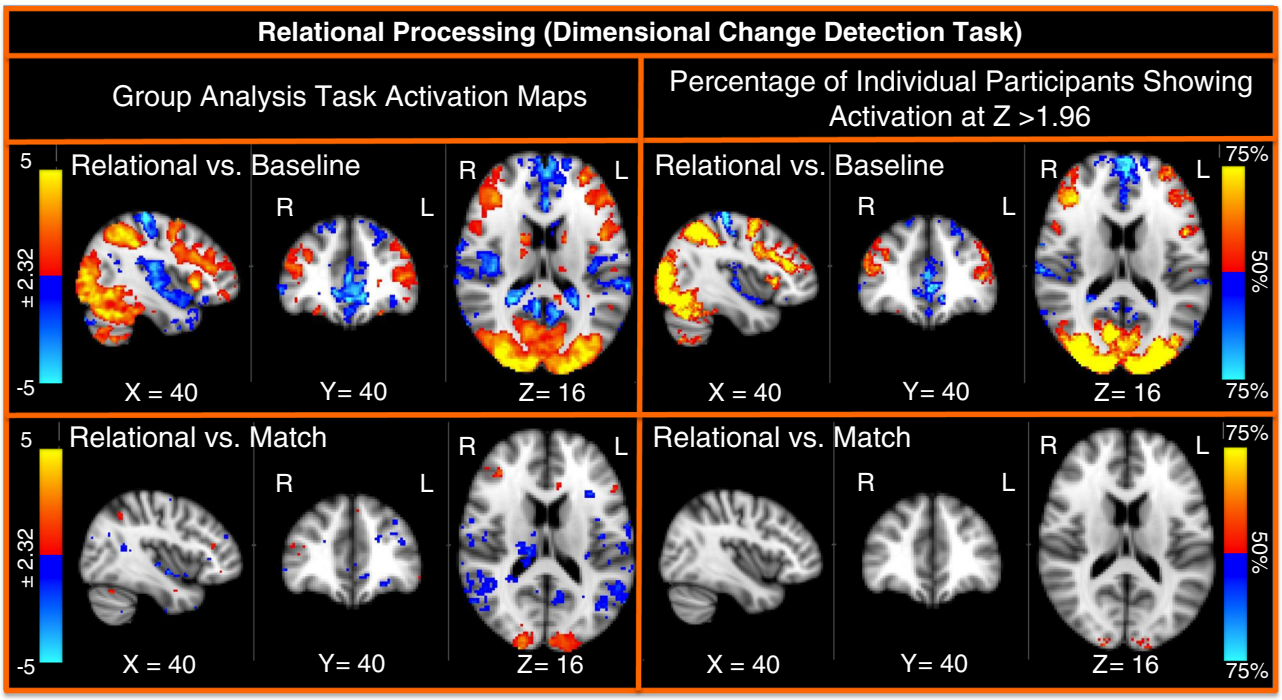

Fig. 10. Group and activation count maps for the relational processing task.

Results

Behavioral data

Toolbox measures

For the majority of the NIH Toolbox measures, the HCP database will report the age-adjusted scaled scores. These scores are based on normative data collected in Phase III of the Toolbox development. The exceptions to this are the Pain Interference, Words in Noise, and the 4-meter Walk Gait Speed measures, for which unadjusted scores are reported, because changes in these measures were made post-norming, preventing the use of the norming data. Fig. 1 shows the distribution of scores for the performance based measures and Table 5 presents the means, medians, range and standard deviations of the self-report measures. This information is provided to illustrate that the sample of subjects to date provides a wide range of scores across all of the measures, which bodes well for their use as individual difference measures.

Non-Toolbox measures

Fig. 2 provides the distribution of scores for the performance based non-Toolbox measures, as well as the internalizing and externalizing dimension scores for the Achenbach Adult Self-Report (as examples). As with the Toolbox measures, we have a good range of scores across all measures.

tfMRI measures

Fig. S1 provides the distribution of accuracy scores for the tfMRI tasks that allow for accuracy assessment. Accuracy is very high in the Hariri Emotion task and the Language task (by design). We also see performance levels in the N-back task consistent with expectations, but also illustrating important variance across the participants. This is also true for the recognition data acquired outside of the scanner. We see good accuracy for the control condition of the relational processing task, and a useful range of performance for the relational condition.

Imaging data

Quality assessment metrics

Fig. S2 displays the distribution of values across our primary quality assessment metrics for the tfMRI data, including all runs for all tasks. Our quality assessment metrics indicate high quality data for the vast majority of runs in these 20 subjects. In fact, the quality of the data provided by these 20 subjects was sufficiently high that we did not exclude any of the runs of those subjects from the analyses presented below. However, of note, we did repeat some runs for some participants when technical problems interfered with scan acquisition at the time of scanning to try to ensure complete data on as many subjects as possible.

Working memory/category specific representations

Fig. 3 shows group level statistical maps for the comparison of 2-back versus baseline and 2-back versus 0-back, as well as maps illustrating the percentage of participants showing activation at $z > 1.96$ (what we refer to as activation count maps (ACMs), see methods for details). As this figure illustrates, the N-back task activates a broad swath of regions thought to be involved in a cognitive control network, including bilateral dorsal and ventral prefrontal cortex, dorsal parietal cortex and dorsal anterior cingulate. Many of these regions are robustly activated within individual participants, even in the contrast of 2-back to 0-back. Further, we also see deactivation in the default mode network, including medial prefrontal cortex, posterior cingulate, and the occipital–parietal junction. In Phase I, we had compared the N-back task to both an event-related and a blocked version of the Posner attention task (see the Supplemental materials for details). The N-back task showed more robust activation of cognitive control and dorsal attention regions than did the modified Posner task, both in the group maps and in the ACMs (Fig. S3). This was true for both versions of the modified Posner, with the event-related version showing overall less robust activation than the blocked version in both the group maps and the ACMs. Fig. 4 shows results for the same 2-back vs. 0-back task contrast as in the lower panels in Fig. 3, but after a grayordinates-based analysis (see

Please cite this article as: Barch, D.M., et al., Function in the human connectome: Task-fMRI and individual differences in behavior, NeuroImage (2013), http://dx.doi.org/10.1016/j.neuroimage.2013.05.033

Methods). Results are displayed on lateral and medial views of the inflated left and right hemisphere surfaces.

Category specific representations

The analyses of the N-back data as a function of stimulus type rather than memory load provide a different pattern of brain activation. Fig. 5 presents both group and ACM maps for the comparison of each stimulus type against baseline, and each stimulus type against the average of all other stimulus types. The later contrast is likely more informative about activation specifically associated with a stimulus type. As can be seen in Fig. 5, the comparison of faces to all other stimulus types identifies bilateral activation in the fusiform face area, the comparison of places to all other stimulus types identifies activation in bilateral parahippocampal place area, and the comparison of body parts to all other stimulus types identifies bilateral activation in extrastriate body areas at the occipital–temporal borders. These activations are clearly identifiable in both the group maps and the ACMs, suggesting that they are robust across subjects. The comparison of places to the other stimulus types in the group maps also identifies activation in primary visual cortex, but this may be related to the larger spatial extent of the place images versus the other image types. The comparison of tools to the other stimulus types did not identify consistent activations selectively associated with visual processing of tools, as we might have expected activations localized to parietal regions.

Incentive processing

Fig. 6 illustrates the data from the gambling task designed to assess reward processing and decision making. As can be seen, many of the expected brain regions are present in the group map of the mostly reward blocks versus baseline, including bilateral striatum and bilateral insula. Fewer regions are present in the group map comparing mostly reward blocks to mostly punishment blocks, though there is some differential activation in striatum and visual cortex. Bilateral insula shows robust and reliable activation across individual subjects in the ACM maps for the reward versus baseline comparison, though only a few voxels are in the striatum in this map. If one looks at a lower threshold, approximately 40% of the subjects do show more extensive activation in the caudate and the putamen. This considerable individual variability in striatal reward response in this guessing task has been found in other studies (Hariri et al., 2006). However, there are no regions that show activation in at least 50% of the participants in the reward versus punishment comparison. In Phase I, we had compared this blocked designed version of the gambling task to a more typical event-related version (see the Supplemental materials for details). As shown in Fig. S4, the blocked and event-related versions showed fairly similar group activation in the reward versus baseline condition, but the blocked version showed greater deactivation. Further, the blocked version showed more consistent activation and deactivation across participants (i.e., ACM maps). In the reward versus punishment condition, both showed activation in the striatum and the medial frontal cortex, though neither showed strong individual subject level activation (ACM maps).

Motor

The activation for the motor mapping task was so strong that we had to use a higher threshold for displaying the group maps, though not the ACMs, to illustrate the differential spatial locations of the activations. The foot versus hand versus tongue activations fall exactly where one would expect them to fall, with the foot superior and on the midline, the hand activations ventral to the foot activations, and the tongue activation ventral to the hand activations (Fig. 7). We also see clear spatial differentiation of the activations in the cerebellum, with the expected ipsilateral representations for left and right hand/foot motion (as compared to the contralateral representations in motor cortex), and bilateral representation of the tongue.

Language processing

Fig. 8 shows the results from both the volume-based analysis displayed on volume slices (top panels) and the grayordinate-based analysis displayed on inflated surfaces (bottom panels). This task elicits robust activation (in both the group maps and the ACMS) in ventral lateral prefrontal cortex and in both superior and inferior temporal cortices, including the anterior temporal poles bilaterally. As to be expected, activation is somewhat stronger on the left than on the right. In Phase I, we had compared this task to a sentence processing task (see the Supplemental materials for details). As shown in Fig. S5, the story processing task developed by Binder and colleagues showed much more robust and extensive activation in superior and anterior temporal cortices than the sentence processing task. This was true when looking both at the group activation maps and at the ACMs.

Social cognition (theory of mind)

The group maps showed activation in a number of regions typically associated with social cognition, including temporal parietal junction and superior temporal cortex regions (Fig. 9). For the temporal parietal and superior temporal regions, this was true for comparison of both the social videos to baseline and the social videos to the random videos. These same regions are seen in the ACMs, demonstrating robust activation in individual subjects. Of note, we also see activation in visual regions typically associated with the processing of both biological and non-biological motion, which led to our not including the

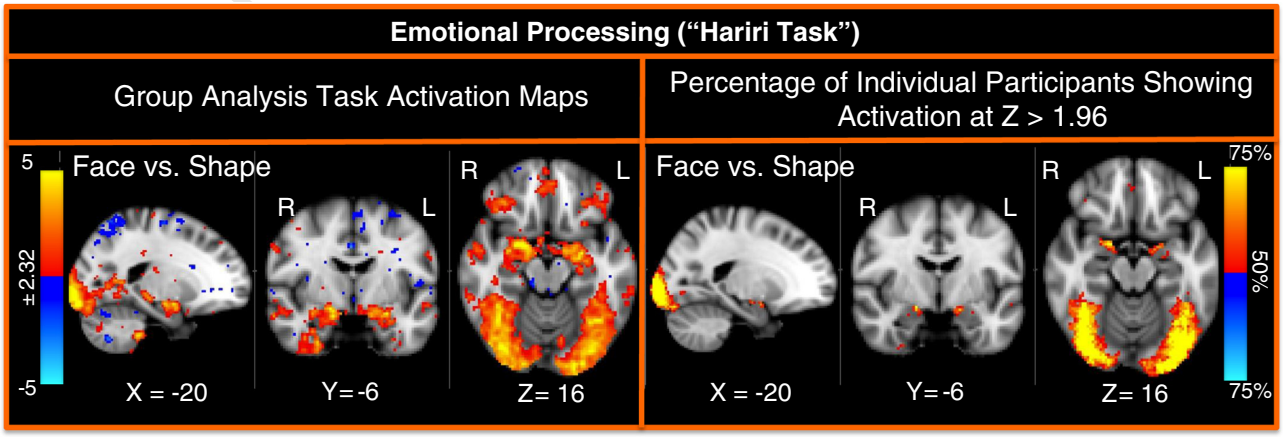

Fig. 11. Group and activation count maps for the emotional processing task.

Please cite this article as: Barch, D.M., et al., Function in the human connectome: Task-fMRI and individual differences in behavior, NeuroImage (2013), http://dx.doi.org/10.1016/j.neuroimage.2013.05.033

separate biological motion task originally piloted in Phase I (see the Supplemental materials for details and Fig. S6).

Relational processing

This task was added in the second stage of Phase I pilot testing because we found that none of the initially piloted tasks provided robust activation in anterior prefrontal cortex. This task elicits consistent activation in bilateral anterior prefrontal cortex in the relational versus baseline comparison, both in the group maps and in the ACMs (Fig. 10). There is less robust activation in the relational versus match comparison, suggesting that the match condition also elicits significant activation in anterior prefrontal cortex.

Emotion processing

There is robust bilateral activation of the amygdala in the emotion processing task, extending into the hippocampus, as well as bilateral activation in medial and lateral orbital frontal cortices (Fig. 11). There is extensive activation of visual regions, including the fusiform face area, which is not surprising given the use of fearful face stimuli. There is also some activation of ventral temporal cortex in the group maps. The ACMs also show bilateral activation of the amygdala and visual cortex including the fusiform, but less consistent activation in orbital frontal or inferior temporal regions in individual subjects. In Phase I, we had compared this task to an IAPS negative versus neutral imaging processing task (see the Supplemental materials for details). The Hariri task elicited more consistent activation in bilateral amygdala regions, which was true when looking both at the group activation maps and at the ACMs (Fig. S7).

Aggregate brain coverage

Fig. 12 shows task count maps for aggregate activations across all contrasts in all tasks, to provide a sense of the overall brain coverage achieved by this set of tasks. These maps show voxels that exhibit activation within an individual subject at $z > 1.96$ for two percentages of participants in a contrast in any task: 50% and 70%. Voxels with no coloring are those that do not show individual subject level activation in that percentage of participants in any contrast for any task. As can be seen, we have excellent coverage of the brain in terms of regions that show activation in at least 50% of the participants in one or more tasks. The primary exception to this is ventral temporal cortex in the area of known susceptibility-related signal dropout. We still have reasonable coverage for regions showing activation in at least 70% of subjects in one or more tasks, though this coverage is less extensive. A similar picture emerges when examining the task count maps that result from the grayordinates-based processing stream (see Fig. 13).

Signal to noise ratio (SNR) maps

As described above, for some tasks we did not see robust activation in some expected regions. Thus, we examined the SNR maps to determine whether low SNR is those regions might be contributing to the absence of activation. The average tSNR maps for each task were very similar in their overall spatial structure; thus Fig. S8 shows the average map for just the Incentive Processing task in the same slices as the map of aggregate brain coverage from the volume-based analysis, and Fig. S9 shows the tSNR map for Incentive

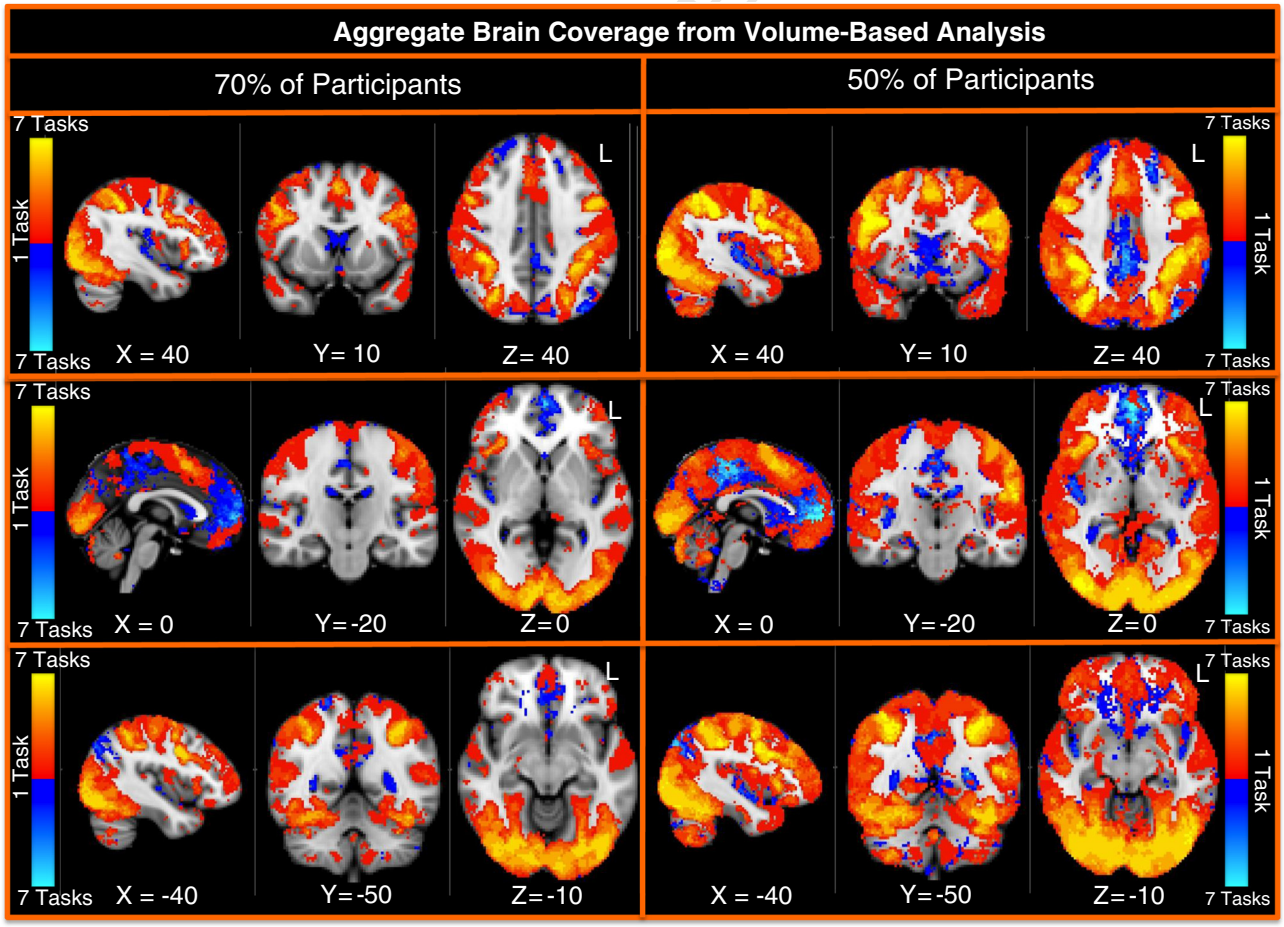

Fig. 12. Task count maps from volume-based analysis. These figures illustrate the number of tasks, for each voxel, that show activation at $z > 1.96$ in at least 70% and 50% of the participants at the individual subject analysis level.

Please cite this article as: Barch, D.M., et al., Function in the human connectome: Task-fMRI and individual differences in behavior, NeuroImage (2013), http://dx.doi.org/10.1016/j.neuroimage.2013.05.033

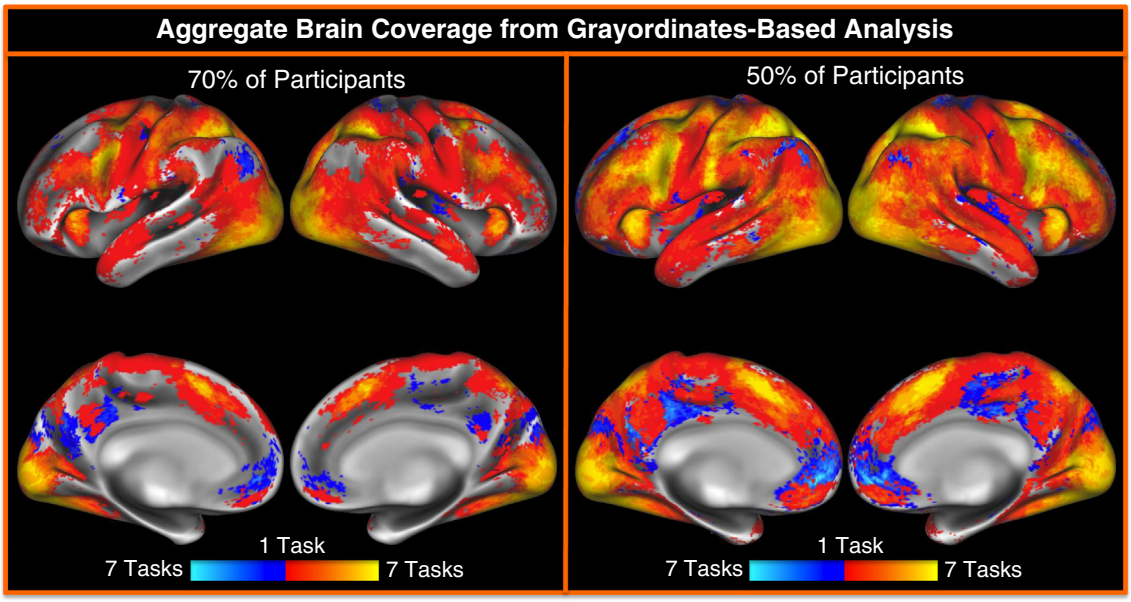

Fig. 13. Task count maps from grayordinates-based analysis. These figures illustrate the number of tasks, for each voxel, that show activation at $z > 1.96$ in at least 70% and 50% of the participants at the individual subject analysis level.

Processing in grayordinate space. As expected, tSNR is highest in the cortical periphery (due to the use of a 32-channel coil) with regions of low tSNR in medial orbitofrontal cortex and inferior temporal cortex due to susceptibility-induced signal dropout in those regions. In addition, tSNR is lower in subcortical regions such as the striatum and the thalamus. The lower tSNR in these regions could be contributing to the less robust individual level subject activation in these regions in the working memory and incentive processing tasks.

Discussion

The goal of this paper was to outline the logic and rationale behind the development of the behavioral, individual differences and task-fMRI batteries and to provide preliminary data on the patterns of activation associated with each of the fMRI tasks, at both group and individual levels. As illustrated by the distribution plots provided for both the Toolbox and non-Toolbox behavioral and self-report measures, we are seeing a good distribution of scores across the vast majority of these measures. This suggest that these measures will be very useful for individual difference analyses that will allow investigators to examine the relationships between variability in performance across a wide array of domains (cognition, emotion, motor, sensory, personality and subthreshold clinical) and individual differences in structural and functional brain connectivity, as well as in task related functional brain activation.

As noted in the Introduction, our goal in the creation of the tfMRI battery was to assess a broad range of functions and processes in a reasonable amount of time so as to elicit brain activation in as many different brain regions and neural systems as possible. Importantly, our focus in designing these tasks was to maximize efficiency and the ability to robustly identify activations at the level of individual subjects. To achieve these goals, the design of the tasks and contrasts was by necessity less fine grained and controlled than one would want if the goal of the battery was to isolate and characterize the specific cognitive or affective processes being supported by different brain regions. As such, we provided data for contrasts that were both more global (e.g., 2-back versus baseline, reward versus baseline) and more focused on isolating specific cognitive processes (e.g., 2-back versus 0-back, reward versus punishment). From our perspective, robust activation in either of these types of contrasts is useful for our purposes of identifying nodes and identifying individual differences in either the spatial location of activation or the magnitude of activation. Although the interpretation of activations in the global contrast may be less clear than the interpretation of activations in the more focused contrast, to the extent that they still provide information about the location and magnitude of activation in brain regions that can be related to structural or functional connectivity, such data is still highly useful to the goal of the HCP. Consistent with this view, the map of aggregate brain activity across any contrast (global or focused) is quite promising, suggesting that our battery of tasks is successful in containing one or more contrasts that identify consistent brain activity in 70% or more of subjects in the same contrast.

Although consistent activation in the majority of the global contrasts will fulfill our purpose in including tfMRI in the HCP protocol, some contrasts (primarily the more focused ones) did not show consistent individual subject level activation. For example, we do not see striatal activation in at least 50% of individual subjects in the comparison of reward versus baseline for the gambling task, we do not see orbital frontal activation in at least 50% of individual subjects in the emotion processing task, we do not see activation in parietal regions in the tools compared to other stimulus types contrast, and we see little individual subject level activation in any brain region in reward versus punishment for gambling or in relational versus match for the relational processing task. These results in part reflect lower tSNR in striatal, thalamic, orbital frontal and anterior temporal regions as compared to other areas of the cortex. As such, these contrasts may not be as useful for examining individual differences in the location of activations based on significance within each subject. However, the data from these contrasts may still be useful in individual level analyses, as we may see reliable variance in the *magnitude* of activation or the spatial location of peak voxels across subjects in specific ROIs that are defined by something other than individual level activation significance testing (e.g., group level and connectivity); such cross-subject variance in activation level (or location) could well still show interesting correlations with non-imaging covariates. Further, all of our testing was done voxel-wise, and it is possible that we will achieve greater sensitivity at the individual subject level using prior information provided by a priori ROIs provided by the parcellation analyses generated using either the resting state or diffusion data, or other approaches that would allow more focused tests. In addition, it is

Please cite this article as: Barch, D.M., et al., Function in the human connectome: Task-fMRI and individual differences in behavior, NeuroImage (2013), http://dx.doi.org/10.1016/j.neuroimage.2013.05.033

possible that individual difference analyses will more clearly identify activation in subcortical regions during tasks such as the incentive processing task, given evidence that individuals high in certain traits or characteristics (e.g., impulsivity, substance use) are more likely to show striatal activation to rewards (Bjork et al., 2008). We also did not see robust medial PFC activation in the social cognition task, which would have been expected based on prior studies. In this case, tSNR was not particularly low in the more dorsal part of medial PFC, though it was lower in subgenual regions. Thus, SNR may not be the sole explanation for the lack of activation in this region in the currently analyzed dataset (n = 20). Alternative analyses that might reveal activation in medial PFC during the social cognition include individual difference approaches, or analyses that code trials as a function of the participant's evaluation of the film clip.

Reliability

The discussion above raises the question of the reliability of the brain activation associated with the different behavioral measures and the brain activation associated with the tfMRI paradigms. The NIH Toolbox measures were chosen in part based on evidence of test–retest reliability in early phase testing, and our selection of non-Toolbox measures was also guided in part by prior evidence of good test–retest reliability. Further, where possible, we selected tfMRI paradigms for piloting based on existing evidence for test–retest reliability, though relatively little data on this property existed for at least some of the domains and measures. In Phase I, we had participants in the first imaging study return two weeks later and examined test–retest reliability, both using traditional ICC measures in group identified ROIs, and using an eta^2 metric (Cohen et al., 2008) to examine the similarity of patterns of activation within subject across time. The ICC values ranged from poor to excellent depending on the task, ROI and contrast, and did not necessarily show a clear pattern that favored one type of task (e.g., blocked versus event-related) or task (e.g., N-back versus Posner) over another. Further, we rapidly realized that the major advances and changes in the pulse sequences and imaging hardware that are being used for Phase II data collection would limit the applicability of any reliability estimates from Phase I as regards the reliability of data being collected in Phase II. Thus, we are collecting a sample of 40 participants who are returning to complete the entire battery approximately 2–4 months after their initial assessment, to provide reliability estimates for all measures to be produced as part of the HCP. These 40 participants will consist of 20 pairs of MZ twins, allowing us to compare across twins within a pair at the same testing point as well as to compare the same twin assessed at two different time points. This data will provide reliability estimates that can be used to modulate interpretations of both individual difference relationships and genetic influences.

Grayordinates-based tfMRI analyses

We illustrated the majority of the results using a volume-based processing stream in order to maximize comparison to prior studies, the majority of which used volume-based processing. However, we also illustrate results from the surface based analyses for tfMRI data that has been implemented by the HCP, and which will eventually be executable within FSL. The principle advantage of surface-based analysis of any kind is in its improvements in spatial localization, both within and across subjects (Fischl et al., 1999a, 1999b, 2008; Frost and Goebel, 2012; Van Essen et al., 2012). Such improvements in spatial localization can be assessed by comparing the spatial extent and boundaries of activations to independent modalities, such as myelin maps (Glasser et al., 2012). Because we planned to make use of surface-based analysis techniques, we used a high-resolution fMRI acquisition (2 mm isotropic), which allows for more specific mapping of fMRI signal from the cortical gray matter ribbon onto the surface (see Glasser et al., this issue). Volume-based analyses may not benefit as much from increases in acquisition resolution, owing to the inherent blurring effects of unconstrained volumetric smoothing. Surface-based analyses also allow direct visualization of activation across the entire cortical sheet without the inaccuracies introduced by mapping volume-averaged data to an average surface (Glasser and Van Essen, 2011; Van Essen et al., 2012). There may also be modest increases in statistical power in surface-based analyses (Anticevic et al., 2008; Tucholka et al., 2012). A future goal of the HCP is to carry out a direct comparison of statistical power and intra-subject alignment for volume-based versus surface-based analyses applied to HCP datasets. Additional advantages are likely to accrue in conjunction with improved surface-based methods for multimodal intersubject alignment based on myelin maps and tfMRI activation maps (Robinson et al., 2013).

Denoising of tfMRI data

Our description of the processing stream for the tfMRI data presented in the current paper did not include any additional denoising steps, such as the inclusion of regressors indexing the degree of movement on each frame (Johnstone et al., 2006), physiological noise modeling (Brooks et al., 2008; Chang and Glover, 2009; Glover et al., 2000), or motion scrubbing (Power et al., 2012; Siegel et al., under review). We compared analyses including each of these additional denoising steps to analyses without any additional denoising in these 20 participants, and did not see any evidence of improvement in terms of either individual level z-statistics or group level z-statistics. We think it highly likely that this lack of improvement with additional denoising steps is related to the high quality of the data from these 20 participants (including low movement). Therefore we plan to reexamine the potential benefits of each of these denoising approaches, as well as an ICA-based approach to denoising, in a larger set of HCP participants that may contain participants with higher levels of movement. Should these analyses indicate that one or more of these additional denoising steps improves the quality of the data, we will modify the HCP tfMRI processing pipeline accordingly.

Conclusion

In summary, we describe here the behavioral, and tfMRI data being collected as part of the primary Phase II HCP protocol. We described the logic and rationale for our choices of tasks and measures for both the behavioral and the imaging components of the study. Preliminary analyses of the first 77 participants to be included in the first quarterly data release indicate a good range of scores on the vast majority of the behavioral measures, boding well for their use in individual difference analyses. We also presented data from 20 subjects (unrelated to each other) to be included in the first quarterly data release. Less-processed data for the other 57 participants will also be released at this time. The data on the 20 participants presented in this paper indicate that we are seeing excellent brain coverage as a whole for our battery of tasks, with the vast majority of tasks eliciting activation in the expected regions at both a group level and in a large percentage of individual subjects. Our next step is to complete the reliability sub-study of Phase II and to present reliability metrics for both the behavioral and the imaging data to guide future interpretation and analyses. Q10

Appendix A. Supplementary data.

Supplementary data to this article can be found online at http://dx.doi.org/10.1016/j.neuroimage.2013.05.033.

Please cite this article as: Barch, D.M., et al., Function in the human connectome: Task-fMRI and individual differences in behavior, NeuroImage (2013), http://dx.doi.org/10.1016/j.neuroimage.2013.05.033

References

Achenbach, T.M., 2009. The Achenbach System of Empirically Based Assessment (ASEBA): Development, Findings, Theory and Applications. University of Vermont Research Center for Children, Youth and Families, Burlington, VT.

Antal, A., Baudewig, J., Paulus, W., Dechent, P., 2008. The posterior cingulate cortex and planum temporale/parietal operculum are activated by coherent visual motion. Vis. Neurosci. 25, 17–26.

Anticevic, A., Dierker, D.L., Gillespie, S.K., Repovs, G., Csernansky, J.G., Van Essen, D.C., Barch, D.M., 2008. Comparing surface-based and volume-based analyses of functional neuroimaging data in patients with schizophrenia. NeuroImage 41, 835–848.

Arditi, A., 2005. Improving the design of the letter contrast sensitivity test. Invest. Ophthalmol. Vis. Sci. 46, 2225–2229.

Bassett, D.S., Bullmore, E.T., Meyer-Lindenberg, A., Apud, J.A., Weinberger, D.R., Coppola, R., 2009. Cognitive fitness of cost-efficient brain functional networks. Proc. Natl. Acad. Sci. U. S. A. 106, 11747–11752.

Beck, R.W., Moke, P.S., Turpin, A.H., Ferris III, F.L., SanGiovanni, J.P., Johnson, C.A., Birch, E.E., Chandler, D.L., Cox, T.A., Blair, R.C., Kraker, R.T., 2003. A computerized method of visual acuity testing: adaptation of the early treatment of diabetic retinopathy study testing protocol. Am. J. Ophthalmol. 135, 194–205.

Bilker, W.B., Hansen, J.A., Brensinger, C.M., Richard, J., Gur, R.E., Gur, R.C., 2012. Development of abbreviated nine-item forms of the Raven's standard progressive matrices test. Assessment 19, 354–369.

Binder, J.R., Gross, W.L., Allendorfer, J.B., Bonilha, L., Chapin, J., Edwards, J.C., Grabowski, T.J., Langfitt, J.T., Loring, D.W., Lowe, M.J., Koenig, K., Morgan, P.S., Ojemann, J.G., Rorden, C., Szaflarski, J.P., Tivarus, M.E., Weaver, K.E., 2011. Mapping anterior temporal lobe language areas with fMRI: a multicenter normative study. NeuroImage 54, 1465–1475.

Bizzi, A., Blasi, V., Falini, A., Ferroli, P., Cadioli, M., Danesi, U., Aquino, D., Marras, C., Caldiroli, D., Broggi, G., 2008. Presurgical functional MR imaging of language and motor functions: validation with intraoperative electrocortical mapping. Radiology 248, 579–589.

Bjork, J.M., Smith, A.R., Hommer, D.W., 2008. Striatal sensitivity to reward deliveries and omissions in substance dependent patients. NeuroImage 42, 1609–1621.

Bracci, S., Ietswaart, M., Peelen, M.V., Cavina-Pratesi, C., 2010. Dissociable neural responses to hands and non-hand body parts in human left extrastriate visual cortex. J. Neurophysiol. 103, 3389–3397.

Brooks, J.C., Beckmann, C.F., Miller, K.L., Wise, R.G., Porro, C.A., Tracey, I., Jenkinson, M., 2008. Physiological noise modelling for spinal functional magnetic resonance imaging studies. NeuroImage 39, 680–692.

Bucholz, K.K., Cadoret, R., Cloninger, C.R., Dinwiddie, S.H., Hesselbrock, V.M., Nurnberger Jr., J.I., Reich, T., Schmidt, I., Schuckit, M.A., 1994. A new, semi-structured psychiatric interview for use in genetic linkage studies: a report on the reliability of the SSAGA. J. Stud. Alcohol 55, 149–158.

Buckner, R.L., Sepulcre, J., Talukdar, T., Krienen, F.M., Liu, H., Hedden, T., Andrews-Hanna, J.R., Sperling, R.A., Johnson, K.A., 2009. Cortical hubs revealed by intrinsic functional connectivity: mapping, assessment of stability, and relation to Alzheimer's disease. J. Neurosci. 29, 1860–1873.

Buckner, R.L., Krienen, F.M., Castellanos, A., Diaz, J.C., Yeo, B.T., 2011. The organization of the human cerebellum estimated by intrinsic functional connectivity. J. Neurophysiol. 106, 2322–2345.

Burgess, G.C., Gray, J.R., Conway, A.R., Braver, T.S., 2011. Neural mechanisms of interference control underlie the relationship between fluid intelligence and working memory span. J. Exp. Psychol. Gen. 140, 674–692.

Buysse, D.J., Reynolds III, C.F., Monk, T.H., Berman, S.R., Kupfer, D.J., 1989. The Pittsburgh Sleep Quality Index: a new instrument for psychiatric practice and research. Psychiatry Res. 28, 193–213.

Caceres, A., Hall, D.L., Zelaya, F.O., Williams, S.C., Mehta, M.A., 2009. Measuring fMRI reliability with the intra-class correlation coefficient. NeuroImage 45, 758–768.

Carter, A.R., Astafiev, S.V., Lang, C.E., Connor, L.T., Rengachary, J., Strube, M.J., Pope, D.L., Shulman, G.L., Corbetta, M., 2010. Resting interhemispheric functional magnetic resonance imaging connectivity predicts performance after stroke. Ann. Neurol. 67, 365–375.

Castelli, F., Happe, F., Frith, U., Frith, C., 2000. Movement and mind: a functional imaging study of perception and interpretation of complex intentional movement patterns. NeuroImage 12, 314–325.

Castelli, F., Frith, C., Happe, F., Frith, U., 2002. Autism, Asperger syndrome and brain mechanisms for the attribution of mental states to animated shapes. Brain 125, 1839–1849.

Chang, C., Glover, G.H., 2009. Effects of model-based physiological noise correction on default mode network anti-correlations and correlations. NeuroImage 47, 1448–1459.

Christoff, K., Prabhakaran, V., Dorfman, J., Zhao, Z., Kroger, J.K., Holyoak, K.J., Gabrieli, J.D., 2001. Rostrolateral prefrontal cortex involvement in relational integration during reasoning. NeuroImage 14, 1136–1149.

Church, J.A., Fair, D.A., Dosenbach, N.U., Cohen, A.L., Miezin, F.M., Petersen, S.E., Schlaggar, B.L., 2009. Control networks in paediatric Tourette syndrome show immature and anomalous patterns of functional connectivity. Brain 132, 225–238.

Cohen, A.L., Fair, D.A., Dosenbach, N.U., Miezin, F.M., Dierker, D., Van Essen, D.C., Schlaggar, B.L., Petersen, S.E., 2008. Defining functional areas in individual human brains using resting functional connectivity MRI. NeuroImage 41, 45–57.

Cole, B.L., 2007. Assessment of inherited colour vision defects in clinical practice. Clin. Exp. Optom. 90, 157–175.

Cole, M.W., Yarkoni, T., Repovs, G., Anticevic, A., Braver, T.S., 2012. Global connectivity of prefrontal cortex predicts cognitive control and intelligence. J. Neurosci. 32, 8988–8999.

Collin, G., Sporns, O., Mandl, R.C., van den Heuvel, M.P., 2013. Structural and functional aspects relating to cost and benefit of rich club organization in the human cerebral cortex. Cereb. Cortex. Q12

Constable, R.T., Ment, L.R., Vohr, B.R., Kesler, S.R., Fulbright, R.K., Lacadie, C., Delancy, S., Katz, K.H., Schneider, K.C., Schafer, R.J., Makuch, R.W., Reiss, A.R., 2008. Prematurely born children demonstrate white matter microstructural differences at 12 years of age, relative to term control subjects: an investigation of group and gender effects. Pediatrics 121, 306–316.

Conway, A.R., Kane, M.J., Bunting, M.F., Hambrick, D.Z., Wilhelm, O., Engle, R.W., 2005. Working memory span tasks: a methodological review and user's guide. Psychon. Bull. Rev. 12, 769–786.

Crum, R.M., Anthony, J.C., Bassett, S.S., Folstein, M.F., 1993. Population-based norms for the Mini-Mental State Examination by age and educational level. JAMA 269, 2386–2391.

Dalley, J.W., Mar, A.C., Economidou, D., Robbins, T.W., 2008. Neurobehavioral mechanisms of impulsivity: fronto-striatal systems and functional neurochemistry. Pharmacol. Biochem. Behav. 90, 250–260.

Delgado, M.R., Nystrom, L.E., Fissell, C., Noll, D.C., Fiez, J.A., 2000. Tracking the hemodynamic responses to reward and punishment in the striatum. J. Neurophysiol. 84, 3072–3077.

Ditman, T., Holcomb, P.J., Kuperberg, G.R., 2007. An investigation of concurrent ERP and self-paced reading methodologies. Psychophysiology 44, 927–935.

Doricchi, F., Macci, E., Silvetti, M., Macaluso, E., 2010. Neural correlates of the spatial and expectancy components of endogenous and stimulus-driven orienting of attention in the Posner task. Cereb. Cortex 20, 1574–1585.

Dougherty, B.E., Flom, R.E., Bullimore, M.A., 2005. An evaluation of the Mars Letter Contrast Sensitivity Test. Optom. Vis. Sci. 82, 970–975.

Downing, P.E., Jiang, Y., Shuman, M., Kanwisher, N., 2001. A cortical area selective for visual processing of the human body. Science 293, 2470–2473.

Downing, P.E., Chan, A.W., Peelen, M.V., Dodds, C.M., Kanwisher, N., 2006. Domain specificity in visual cortex. Cereb. Cortex 16, 1453–1461.

Downing, P.E., Peelen, M.V., Wiggett, A.J., Tew, B.D., 2006. The role of the extrastriate body area in action perception. Soc. Neurosci. 1, 52–62.

Drobyshevsky, A., Baumann, S.B., Schneider, W., 2006. A rapid fMRI task battery for mapping of visual, motor, cognitive, and emotional function. NeuroImage 31, 732–744.

Duncan, J., 2003. Intelligence tests predict brain response to demanding task events. Nat. Neurosci. 6, 207–208.

Duncan, J., 2005. Frontal lobe function and general intelligence: why it matters. Cortex 41, 215–217.

Duncan, J., Seltz, R.J., Kolodny, J., Bor, D., Herzog, H., Ahmed, A., Newell, F.N., Emslie, H., 2000. A neural basis for general intelligence. Am. J. Ophthalmol. 130, 687.

Engelmann, J.B., Damaraju, E., Padmala, S., Pessoa, L., 2009. Combined effects of attention and motivation on visual task performance: transient and sustained motivational effects. Front. Hum. Neurosci. 3, 4.

Estle, S.J., Green, L., Myerson, J., Holt, D.D., 2006. Differential effects of amount on temporal and probability discounting of gains and losses. Mem. Cognit. 34, 914–928.

Fair, D.A., Dosenbach, N.U., Church, J.A., Cohen, A.L., Brahmbhatt, S., Miezin, F.M., Barch, D.M., Raichle, M.E., Petersen, S.E., Schlaggar, B.L., 2007. Development of distinct control networks through segregation and integration. Proc. Natl. Acad. Sci. 104, 13507–13512.

Fair, D.A., Cohen, A.L., Power, J.D., Dosenbach, N.U., Church, J.A., Miezin, F.M., Schlaggar, B.L., Petersen, S.E., 2009. Functional brain networks develop from a "local to distributed" organization. PLoS Comput. Biol. 5, e1000381.

Fair, D.A., Nigg, J.T., Iyer, S., Bathula, D., Mills, K.L., Dosenbach, N.U., Schlaggar, B.L., Mennes, M., Gutman, D., Bangaru, S., Buitelaar, J.K., Dickstein, D.P., Di Martino, A., Kennedy, D.N., Kelly, C., Luna, B., Schweitzer, J.B., Velanova, K., Wang, Y.F., Mostofsky, S., Castellanos, F.X., Milham, M.P., 2012. Distinct neural signatures detected for ADHD subtypes after controlling for micro-movements in resting state functional connectivity MRI data. Front. Syst. Neurosci. 6, 80.

Feinberg, D.A., Moeller, S., Smith, S.M., Auerbach, E., Ramanna, S., Glasser, M.F., Miller, K.L., Ugurbil, K., Yacoub, E., 2010. Multiplexed echo planar imaging for sub-second whole brain FMRI and fast diffusion imaging. PLoS One 5, e15710.

Fischl, B., Sereno, M.I., Dale, A.M., 1999. Cortical surface-based analysis. II: inflation, flattening, and a surface-based coordinate system. NeuroImage 9, 195–207.

Fischl, B., Sereno, M.I., Tootell, R.B., Dale, A.M., 1999. High-resolution intersubject averaging and a coordinate system for the cortical surface. Hum. Brain Mapp. 8, 272–284.

Fischl, B., Rajendran, N., Busa, E., Augustinack, J., Hinds, O., Yeo, B.T., Mohlberg, H., Amunts, K., Zilles, K., 2008. Cortical folding patterns and predicting cytoarchitecture. Cereb. Cortex 18, 1973–1980.

Fitzsimmons, J., Kubicki, M., Shenton, M.E., 2013. Review of functional and anatomical brain connectivity findings in schizophrenia. Curr. Opin. Psychiatry. Q13

Folstein, M.F., Folstein, S.E., McHugh, P.R., 1975. Mini-mental state: a practical method for grading the cognitive state of patients for the clinician. J. Psychiatr. Res. 12, 189–198.

Forbes, E.E., Hariri, A.R., Martin, S.L., Silk, J.S., Moyles, D.L., Fisher, P.M., Brown, S.M., Ryan, N.D., Birmaher, B., Axelson, D.A., Dahl, R.E., 2009. Altered striatal activation predicting real-world positive affect in adolescent major depressive disorder. Am. J. Psychiatry 166, 64–73.

Fornito, A., Zalesky, A., Pantelis, C., Bullmore, E.T., 2012. Schizophrenia, neuroimaging and connectomics. NeuroImage 62, 2296–2314.

Fox, C.J., Iaria, G., Barton, J.J., 2009. Defining the face processing network: optimization of the functional localizer in fMRI. Hum. Brain Mapp. 30, 1637–1651.

Frost, M.A., Goebel, R., 2012. Measuring structural–functional correspondence: spatial variability of specialized brain regions after macros-anatomical alignment. NeuroImage 59, 1369–1381.

Please cite this article as: Barch, D.M., et al., Function in the human connectome: Task-fMRI and individual differences in behavior, NeuroImage (2013), http://dx.doi.org/10.1016/j.neuroimage.2013.05.033

Glasser, M.F., Van Essen, D.C., 2011. Mapping human cortical areas in vivo based on myelin content as revealed by T1- and T2-weighted MRI. J. Neurosci. 31, 11597–11616.

Glasser, M.F., Burgess, G.C., Xu, J., He, Y., Barch, D.M., Coalson, T.S., Fischl, B., Harms, M.P., Jenkinson, M., Patenaude, B., Petersen, S.E., Schlaggar, B.L., Smith, S., Woolrich, M.W., Yacoub, E., Van Essen, D., 2012. Surface Gradient Comparison of Myelin and fMRI: Architectonic and Functional Border Co-localization. Organization for Human Brain Mapping, Beijing, China.

Glasser, M.F., Sotiropoulos, S.N., Wilson, J.A., Coalson, T.S., Fischl, B., Andersson, J.L., Xu, J., Jbadbi, S., Webster, M., Polimeni, J.R., Van Essen, D.C., Jenkinson, M., Consortium, f.t.W.-M.H., 2013. The minimal preprocessing pipelines for the Human Connectome Project. NeuroImage (this issue, Special Issue "Mapping the Connectome"). Q14

Glover, G.H., 1999. Deconvolution of impulse response in event-related BOLD fMRI. NeuroImage 9, 416–429.

Glover, G.H., Li, T.Q., Ress, D., 2000. Image-based method for retrospective correction of physiological motion effects in fMRI: RETROICOR. Magn. Reson. Med. 44, 162–167.

Goldberg, L.R., 1993. The structure of phenotypic personality traits. Am. Psychol. 48, 26–34.

Gountouna, V.E., Job, D.E., McIntosh, A.M., Moorhead, T.W., Lymer, G.K., Whalley, H.C., Hall, J., Waiter, G.D., Brennan, D., McGonigle, D.J., Ahearn, T.S., Cavanagh, J., Condon, B., Hadley, D.M., Marshall, I., Murray, A.D., Steele, J.D., Wardlaw, J.M., Lawrie, S.M., 2009. Functional Magnetic Resonance Imaging (fMRI) reproducibility and variance components across visits and scanning sites with a finger tapping task. NeuroImage. Q15

Gozzo, Y., Vohr, B., Lacadie, C., Hampson, M., Katz, K.H., Maller-Kesselman, J., Schneider, K.C., Peterson, B.S., Rajeevan, N., Makuch, R.W., Constable, R.T., Ment, L.R., 2009. Alterations in neural connectivity in preterm children at school age. NeuroImage 48, 458–463.

Gray, J.R., Chabris, C.F., Braver, T.S., 2003. Neural mechanisms of general fluid intelligence. Nat. Neurosci. 6, 316–322.

Gray, J.R., Burgess, G.C., Schaefer, A., Yarkoni, T., Larsen, R.J., Braver, T.S., 2005. Affective personality differences in neural processing efficiency confirmed using fMRI. Cogn. Affect. Behav. Neurosci. 5, 182–190.

Green, L., Myerson, J., Shah, A.K., Estle, S.J., Holt, D.D., 2007. Do adjusting-amount and adjusting-delay procedures produce equivalent estimates of subjective value in pigeons? J. Exp. Anal. Behav. 87, 337–347.

Gur, R.C., Ragland, J.D., Moberg, P.J., Bilker, W.B., Kohler, C., Siegel, S.J., Gur, R.E., 2001. Computerized neurocognitive scanning: II. The profile of schizophrenia. Neuropsychopharmacology 25, 777–788.

Gur, R.C., Ragland, J.D., Moberg, P.J., Turner, T.H., Bilker, W.B., Kohler, C., Siegel, S.J., Gur, R.E., 2001. Computerized neurocognitive scanning: I. Methodology and validation in healthy people. Neuropsychopharmacology 25, 766–776.

Gur, R.C., Richard, J., Hughett, P., Calkins, M.E., Macy, L., Bilker, W.B., Brensinger, C., Gur, R.E., 2010. A cognitive neuroscience-based computerized battery for efficient measurement of individual differences: standardization and initial construct validation. J. Neurosci. Methods 187, 254–262.

Hariri, A.R., Tessitore, A., Mattay, V.S., Fera, F., Weinberger, D.R., 2002. The amygdala response to emotional stimuli: a comparison of faces and scenes. NeuroImage 17, 317–323.

Hariri, A.R., Brown, S.M., Williamson, D.E., Flory, J.D., de Wit, H., Manuck, S.B., 2006. Preference for immediate over delayed rewards is associated with magnitude of ventral striatal activity. J. Neurosci. 26, 13213–13217.

Harriger, L., van den Heuvel, M.P., Sporns, O., 2012. Rich club organization of macaque cerebral cortex and its role in network communication. PLoS One 7, e46497.

Hawellek, D.J., Hipp, J.F., Lewis, C.M., Corbetta, M., Engel, A.K., 2011. Increased functional connectivity indicates the severity of cognitive impairment in multiple sclerosis. Proc. Natl. Acad. Sci. U. S. A. 108, 19066–19071.

Haymes, S.A., Roberts, K.F., Cruess, A.F., Nicolela, M.T., LeBlanc, R.P., Ramsey, M.S., Chauhan, B.C., Artes, P.H., 2006. The letter contrast sensitivity test: clinical evaluation of a new design. Invest. Ophthalmol. Vis. Sci. 47, 2739–2745.

He, B.J., Snyder, A.Z., Vincent, J.L., Epstein, A., Shulman, G.L., Corbetta, M., 2007. Breakdown of functional connectivity in frontoparietal networks underlies behavioral deficits in spatial neglect. Neuron 53, 905–918.

He, Y., Dagher, A., Chen, Z., Charil, A., Zijdenbos, A., Worsley, K., Evans, A., 2009. Impaired small-world efficiency in structural cortical networks in multiple sclerosis associated with white matter lesion load. Brain. Q16

Heatherton, T.F., Kozlowski, L.T., Frecker, R.C., Fagerstrom, K.O., 1991. The Fagerstrom Test for Nicotine Dependence: a revision of the Fagerstrom Tolerance Questionnaire. Br. J. Addict. 86, 1119–1127.

Heine, S.J., Buchtel, E.E., 2009. Personality: the universal and the culturally specific. Annu. Rev. Psychol. 60, 369–394.

Hesselbrock, M., Easton, C., Bucholz, K.K., Schuckit, M., Hesselbrock, V., 1999. A validity study of the SSAGA—a comparison with the SCAN. Addiction 94, 1361–1370.

Hirsch, J., Ruge, M.I., Kim, K.H., Correa, D.D., Victor, J.D., Relkin, N.R., Labar, D.R., Krol, G., Bilsky, M.H., Souweidane, M.M., DeAngelis, L.M., Gutin, P.H., 2000. An integrated functional magnetic resonance imaging procedure for preoperative mapping of cortical areas associated with tactile, motor, language, and visual functions. Neurosurgery 47, 711–721 (discussion 721-712).

Hulvershorn, L.A., Cullen, K., Anand, A., 2011. Toward dysfunctional connectivity: a review of neuroimaging findings in pediatric major depressive disorder. Brain Imaging Behav. 5, 307–328.

Hwang, K., Hallquist, M.N., Luna, B., 2012. The development of hub architecture in the human functional brain network. Cereb. Cortex. Q17

Imperati, D., Colcombe, S., Kelly, C., Di Martino, A., Zhou, J., Castellanos, F.X., Milham, M.P., 2011. Differential development of human brain white matter tracts. PLoS One 6, e23437.

Insel, T.R., 2008. Assessing the economic costs of serious mental illness. Am. J. Psychiatry 165, 663–665.

Johnstone, T., Ores Walsh, K.S., Greischar, L.L., Alexander, A.L., Fox, A.S., Davidson, R.J., Oakes, T.R., 2006. Motion correction and the use of motion covariates in multiple-subject fMRI analysis. Hum. Brain Mapp. 27, 779–788.

Kanwisher, N., 2001. Faces and places: of central (and peripheral) interest. Nat. Neurosci. 4, 455–456.

Kawabata Duncan, K.J., Devlin, J.T., 2011. Improving the reliability of functional localizers. NeuroImage 57, 1022–1030.

Kozlowski, L.T., Porter, C.Q., Orleans, C.T., Pope, M.A., Heatherton, T., 1994. Predicting smoking cessation with self-reported measures of nicotine dependence: FTQ, FTND, and HSI. Drug Alcohol Depend. 34, 211–216.

Kung, C.C., Peissig, J.J., Tarr, M.J., 2007. Is region-of-interest overlap comparison a reliable measure of category specificity? J. Cogn. Neurosci. 19, 2019–2034.

Kuperberg, G.R., Sitnikova, T., Lakshmanan, B.M., 2008. Neuroanatomical distinctions within the semantic system during sentence comprehension: evidence from functional magnetic resonance imaging. NeuroImage 40, 367–388.

Larson-Prior, L., Oostenveld, R., Della Penna, S., Michalareas, G., Prior, F., Babajani-Feremi, A., Schoffelen, J.M., Marzetti, L., de Pasquale, F., Di Pompeo, F., Stout, J., Woolrich, M.W., Luo, Q., Bucholz, R., Fries, P., Pizzella, V., Romani, G.L., Corbetta, M., Snyder, A.Z., Consortium, f.t.W.-M.H., 2013. Adding dynamics to the Human Connectome Project with MEG. NeuroImage (this issue, Special Issue "Mapping the Connectome"). Q18

Li, Y., Liu, Y., Li, J., Qin, W., Li, K., Yu, C., Jiang, T., 2009. Brain anatomical network and intelligence. PLoS Comput. Biol. 5, e1000395.

Liu, T.T., Frank, L.R., Wong, E.C., Buxton, R.B., 2001. Detection power, estimation efficiency, and predictability in event-related fMRI. NeuroImage 13, 759–773.

Manuck, S.B., Brown, S.M., Forbes, E.E., Hariri, A.R., 2007. Temporal stability of individual differences in amygdala reactivity. Am. J. Psychiatry 164, 1613–1614. Q19

Marcus, D.S., Harms, M.P., Snyder, A.M., Jenkinson, M., Wilson, J.T., Glasser, M.F., Barch, D.M., Archie, K.A., Burgess, G.C., Ramaratnam, M., Hodge, M., Horton, W., Herrick, R., Olsen, T., Mckay, M., House, M., Hileman, M., Reid, E., Harwell, J., Coalson, T., Schindler, J., Elam, J., Curtis, C.W., Van Essen, D.C., 2013. Human Connectome Project informatics: quality control, database services and data visualization. NeuroImage (this issue, Special Issue "Mapping the Connectome"). Q20

May, J.C., Delgado, M.R., Dahl, R.E., Stenger, V.A., Ryan, N.D., Fiez, J.A., Carter, C.S., 2004. Event-related functional magnetic resonance imaging of reward-related brain circuitry in children and adolescents. Biol. Psychiatry 55, 359–366.

McCrae, R.R., Costa Jr., P.T., 2004. A contemplated revision of the NEO Five Factor Inventory. Personal. Individ. Differ. 36, 587–596.

McCrae, R.R., Costa Jr., P.T., 2008. The five factor theory of personality. In: John, O.P., Robins, R.W., Pervin, L.A. (Eds.), Handbook of Personality: Theory and Research. Guilford, New York, pp. 159–181.

Miller, M.B., Van Horn, J.D., Wolford, G.L., Handy, T.C., Valsangkar-Smyth, M., Inati, S., Grafton, S., Gazzaniga, M.S., 2002. Extensive individual differences in brain activations associated with episodic retrieval are reliable over time. J. Cogn. Neurosci. 14, 1200–1214.

Miller, M.B., Donovan, C.L., Van Horn, J.D., German, E., Sokol-Hessner, P., Wolford, G.L., 2009. Unique and persistent individual patterns of brain activity across different memory retrieval tasks. NeuroImage 48, 625–635.

Moeller, S., Yacoub, E., Olman, C.A., Auerbach, E., Strupp, J., Harel, N., Ugurbil, K., 2010. Multiband multislice GE-EPI at 7 Tesla, with 16-fold acceleration using partial parallel imaging with application to high spatial and temporal whole-brain fMRI. Magn. Reson. Med. 63, 1144–1153.

Moke, P.S., Turpin, A.H., Beck, R.W., Holmes, J.M., Repka, M.X., Birch, E.E., Hertle, R.W., Kraker, R.T., Miller, J.M., Johnson, C.A., 2001. Computerized method of visual acuity testing: adaptation of the amblyopia treatment study visual acuity testing protocol. Am. J. Ophthalmol. 132, 903–909.

Morioka, T., Yamamoto, T., Mizushima, A., Tombimatsu, S., Shigeto, H., Hasuo, K., Nishio, S., Fujii, K., Fukui, M., 1995. Comparison of magnetoencephalography, functional MRI, and motor evoked potentials in the localization of the sensory–motor cortex. Neurol. Res. 17, 361–367.

Mullen, K.M., Vohr, B.R., Katz, K.H., Schneider, K.C., Lacadie, C., Hampson, M., Makuch, R.W., Reiss, A.L., Constable, R.T., Ment, L.R., 2011. Preterm birth results in alterations in neural connectivity at age 16 years. NeuroImage 54, 2563–2570.

Myerson, J., Green, L., Warusawitharana, M., 2001. Area under the curve as a measure of discounting. J. Exp. Anal. Behav. 76, 235–243.

Nelson, S.M., Cohen, A.L., Power, J.D., Wig, G.S., Miezin, F.M., Wheeler, M.E., Velanova, K., Donaldson, D.I., Phillips, J.S., Schlaggar, B.L., Petersen, S.E., 2010. A parcellation scheme for human left lateral parietal cortex. Neuron 67, 156–170.

O'Craven, K.M., Kanwisher, N., 2000. Mental imagery of faces and places activates corresponding stimulus-specific brain regions. J. Cogn. Neurosci. 12, 1013–1023.

Oldfield, R.C., 1971. The assessment and analysis of handedness: the Edinburgh inventory. Neuropsychologia 9, 97–113.

Panigrahy, A., Wisnowski, J.L., Furtado, A., Lepore, N., Paquette, L., Bluml, S., 2012. Neuroimaging biomarkers of preterm brain injury: toward developing the preterm connectome. Pediatr. Radiol. 42 (Suppl. 1), S33–S61.

Park, S., Chun, M.M., 2009. Different roles of the parahippocampal place area (PPA) and retrosplenial cortex (RSC) in panoramic scene perception. NeuroImage 47, 1747–1756.

Peelen, M.V., Downing, P.E., 2005. Within-subject reproducibility of category-specific visual activation with functional MRI. Hum. Brain Mapp. 25, 402–408.

Peuskens, H., Vanrie, J., Verfaillie, K., Orban, G.A., 2005. Specificity of regions processing biological motion. Eur. J. Neurosci. 21, 2864–2875.

Phan, K.L., Fitzgerald, D.A., Gao, K., Moore, G.J., Tancer, M.E., Posse, S., 2004. Real-time fMRI of cortico-limbic brain activity during emotional processing. Neuroreport 15, 527–532.

Please cite this article as: Barch, D.M., et al., Function in the human connectome: Task-fMRI and individual differences in behavior, NeuroImage (2013), http://dx.doi.org/10.1016/j.neuroimage.2013.05.033

Pinsk, M.A., Arcaro, M., Weiner, K.S., Kalkus, J.F., Inati, S.J., Gross, C.G., Kastner, S., 2009. Neural representations of faces and body parts in macaque and human cortex: a comparative FMRI study. J. Neurophysiol. 101, 2581–2600.

Power, J.D., Barnes, K.A., Snyder, A.Z., Schlaggar, B.L., Petersen, S.E., 2012. Spurious but systematic correlations in functional connectivity MRI networks arise from subject motion. NeuroImage 59, 2142–2154.

Prabhakaran, V., Smith, J.A., Desmond, J.E., Glover, G.H., Gabrieli, J.D., 1997. Neural substrates of fluid reasoning: an fMRI study of neocortical activation during performance of the Raven's Progressive Matrices Test. Cogn. Psychol. 33, 43–63.

Repovs, G., Csernansky, J.G., Barch, D.M., 2011. Brain network connectivity in individuals with schizophrenia and their siblings. Biol. Psychiatry 69, 967–973.

Robinson, E.C., Jbabdi, S., Andersson, J., Smith, S., Glasser, M.F., Van Essen, D., Burgess, G.C., Harms, M.P., Jenkinson, M., 2013. Multimodal surface matching: a new surface registration approach that improves functional alignment. Organization of Human Brain Mapping, Seattle, Washington, USA.

Rocca, M.A., Absinta, M., Valsasina, P., Ciccarelli, O., Marino, S., Rovira, A., Gass, A., Wegner, C., Enzinger, C., Korteweg, T., Sormani, M.P., Mancini, L., Thompson, A.J., De Stefano, N., Montalban, X., Hirsch, J., Kappos, L., Ropele, S., Palace, J., Barkhof, F., Matthews, P.M., Filippi, M., 2009. Abnormal connectivity of the sensorimotor network in patients with MS: a multicenter fMRI study. Hum. Brain Mapp. 30, 2412–2425.

Saxe, R., Jamal, N., Powell, L., 2006. My body or yours? The effect of visual perspective on cortical body representations. Cereb. Cortex 16, 178–182.

Schafer, R.J., Lacadie, C., Vohr, B., Kesler, S.R., Katz, K.H., Schneider, K.C., Pugh, K.R., Makuch, R.W., Reiss, A.L., Constable, R.T., Ment, L.R., 2009. Alterations in functional connectivity for language in prematurely born adolescents. Brain 132, 661–670.

Schoonheim, M.M., Geurts, J.J., Landi, D., Douw, L., van der Meer, M.L., Vrenken, H., Polman, C.H., Barkhof, F., Stam, C.J., 2013. Functional connectivity changes in multiple sclerosis patients: a graph analytical study of MEG resting state data. Hum. Brain Mapp. 34, 52–61.

Shamosh, N.A., Deyoung, C.G., Green, A.E., Reis, D.L., Johnson, M.R., Conway, A.R., Engle, R.W., Braver, T.S., Gray, J.R., 2008. Individual differences in delay discounting: relation to intelligence, working memory, and anterior prefrontal cortex. Psychol. Sci. 19, 904–911.

Siegel, J.S., Power, J.D., Vogel, A.C., Church, J.A., Dubis, J.W., Schlaggar, B.L., Petersen, S.E., 2013. Statistical Improvements in fMRI Analyses Produced by Censoring High Motion Datapoints (under review). Q21

Smith, R., Keramatian, K., Christoff, K., 2007. Localizing the rostrolateral prefrontal cortex at the individual level. NeuroImage 36, 1387–1396.

Song, M., Zhou, Y., Li, J., Liu, Y., Tian, L., Yu, C., Jiang, T., 2008. Brain spontaneous functional connectivity and intelligence. NeuroImage 41, 1168–1176.

Stevens, M.C., Skudlarski, P., Pearlson, G.D., Calhoun, V.D., 2009. Age-related cognitive gains are mediated by the effects of white matter development on brain network integration. NeuroImage 48, 738–746.

Strakowski, S.M., Adler, C.M., Almeida, J., Altshuler, L.L., Blumberg, H.P., Chang, K.D., DelBello, M.P., Frangou, S., McIntosh, A., Phillips, M.L., Sussman, J.E., Townsend, J.D., 2012. The functional neuroanatomy of bipolar disorder: a consensus model. Bipolar Disord. 14, 313–325.

Supekar, K., Musen, M., Menon, V., 2009. Development of large-scale functional brain networks in children. PLoS Biol. 7, e1000157.

Sutherland, M.T., McHugh, M.J., Pariyadath, V., Stein, E.A., 2012. Resting state functional connectivity in addiction: lessons learned and a road ahead. NeuroImage 62, 2281–2295.

Taylor, J.C., Wiggett, A.J., Downing, P.E., 2007. Functional MRI analysis of body and body part representations in the extrastriate and fusiform body areas. J. Neurophysiol. 98, 1626–1633.

Thayaparan, K., Crossland, M.D., Rubin, G.S., 2007. Clinical assessment of two new contrast sensitivity charts. Br. J. Ophthalmol. 91, 749–752.

Tricomi, E.M., Delgado, M.R., Fiez, J.A., 2004. Modulation of caudate activity by action contingency. Neuron 41, 281–292.

Tucholka, A., Fritsch, V., Poline, J.B., Thirion, B., 2012. An empirical comparison of surface-based and volume-based group studies in neuroimaging. NeuroImage 63, 1443–1453.

Ugurbil, K., Xu, J., Auerbach, E.J., Moeller, S., Vu, A., Duarte-Carvajalino, J., Lenglet, C., Wu, X., Schmitter, S., Van de Moortele, P.F., Strupp, J., Sapiro, G., De Martino, F., Wang, D., Harel, N., Garwood, M., Chen, L., Feinberg, D.A., Smith, S.A., Miller, K.L., Sotriopoulos, S.N., Jbadbi, S., Andersson, J.L., Behrens, T.J., Glasser, M.F., Van Essen, D.C., Yacoub, E., Consortium, f.t.W.-M.H., 2013. Pushing spatial and temporal resolution for functional and diffusion weighted imaging in the Human Connectome Project. NeuroImage (in press, Special Issue "Mapping the Connectome"). Q22

van den Heuvel, M.P., Sporns, O., 2011. Rich-club organization of the human connectome. J. Neurosci. 31, 15775–15786.

van den Heuvel, M.P., Stam, C.J., Kahn, R.S., Hulshoff Pol, H.E., 2009. Efficiency of functional brain networks and intellectual performance. J. Neurosci. 29, 7619–7624.

Van Essen, D.C., Ugurbil, K., Auerbach, E., Barch, D., Behrens, T.E., Bucholz, R., Chang, A., Chen, L., Corbetta, M., Curtiss, S.W., Della Penna, S., Feinberg, D., Glasser, M.F., Harel, N., Heath, A.C., Larson-Prior, L., Marcus, D., Michalareas, G., Moeller, S., Oostenveld, R., Petersen, S.E., Prior, F., Schlaggar, B.L., Smith, S.M., Snyder, A.Z., Xu, J., Yacoub, E., 2012. The Human Connectome Project: a data acquisition perspective. NeuroImage. Q23

Van Essen, D., Smith, S.M., Barch, D.M., Behrens, T.E., Yacoub, E., Ugurbil, K., Consortium, F.t.W.-M.H., 2013. The WU-Minn Human Connectome Project: an overview. NeuroImage (in press, Special Issue "Mapping the Connectome"). Q24

Vissers, M.E., Cohen, M.X., Geurts, H.M., 2012. Brain connectivity and high functioning autism: a promising path of research that needs refined models, methodological convergence, and stronger behavioral links. Neurosci. Biobehav. Rev. 36, 604–625.

Warnking, J., Dojat, M., Guerin-Dugue, A., Delon-Martin, C., Olympieff, S., Richard, N., Chehikian, A., Segebarth, C., 2002. fMRI retinotopic mapping—step by step. NeuroImage 17, 1665–1683.

Wendelken, C., Nakhabenko, D., Donohue, S.E., Carter, C.S., Bunge, S.A., 2008. "Brain is to thought as stomach is to ??": investigating the role of rostrolateral prefrontal cortex in relational reasoning. J. Cogn. Neurosci. 20, 682–693.

Wheatley, T., Milleville, S.C., Martin, A., 2007. Understanding animate agents: distinct roles for the social network and mirror system. Psychol. Sci. 18, 469–474.

White, S.J., Coniston, D., Rogers, R., Frith, U., 2011. Developing the Frith–Happe animations: a quick and objective test of Theory of Mind for adults with autism. Autism Res. 4, 149–154.

Whitfield-Gabrieli, S., Ford, J.M., 2012. Default mode network activity and connectivity in psychopathology. Annu. Rev. Clin. Psychol. 8, 49–76.

Wierenga, C.E., Perlstein, W.M., Benjamin, M., Leonard, C.M., Rothi, L.G., Conway, T., Cato, M.A., Gopinath, K., Briggs, R., Crosson, B., 2009. Neural substrates of object identification: functional magnetic resonance imaging evidence that category and visual attribute contribute to semantic knowledge. J. Int. Neuropsychol. Soc. 15, 169–181.

Woolrich, M.W., Ripley, B.D., Brady, M., Smith, S.M., 2001. Temporal autocorrelation in univariate linear modeling of FMRI data. NeuroImage 14, 1370–1386.

Worbe, Y., Malherbe, C., Hartmann, A., Pelegrini-Issac, M., Messe, A., Vidailhet, M., Lehericy, S., Benali, H., 2012. Functional immaturity of cortico-basal ganglia networks in Gilles de la Tourette syndrome. Brain 135, 1937–1946.

Yeo, B.T., Krienen, F.M., Sepulcre, J., Sabuncu, M.R., Lashkari, D., Hollinshead, M., Roffman, J.L., Smoller, J.W., Zollei, L., Polimeni, J.R., Fischl, B., Liu, H., Buckner, R.L., 2011. The organization of the human cerebral cortex estimated by intrinsic functional connectivity. J. Neurophysiol. 106, 1125–1165.

Zuo, X.N., Kelly, C., Di Martino, A., Mennes, M., Margulies, D.S., Bangaru, S., Grzadzinski, R., Evans, A.C., Zang, Y.F., Castellanos, F.X., Milham, M.P., 2010. Growing together and growing apart: regional and sex differences in the lifespan developmental trajectories of functional homotopy. J. Neurosci. 30, 15034–15043.

Please cite this article as: Barch, D.M., et al., Function in the human connectome: Task-fMRI and individual differences in behavior, NeuroImage (2013), http://dx.doi.org/10.1016/j.neuroimage.2013.05.033